

Water Flow Optimization Algorithm: A Nature-Inspired Metaheuristic Based on Plant Water Transport Mechanisms

Hector Carreon-Ortiz, Fevrier Valdez*, Oscar Castillo

Tijuana Institute of Technology/TecNM, Tijuana,
Mexico

fevrier@tectijuana.mx

Abstract. In this work we present the Water Flow Optimization Algorithm (WFOA), a nature-inspired metaheuristic based on the transport of water in plants driven by transpiration, cohesion–tension and water-potential gradients. WFOA models the “flow” of solutions from roots to leaves through a simple transport process in which an adaptive flow equation moves candidate solutions toward promising regions, while random perturbations and boundary handling keep the population diverse. To analyze its behavior, we tested WFOA on 36 classical benchmark functions with several dimensionalities (30, 50, and 100 variables). Each problem was run 30 times independently under a fixed evaluation budget. Performance was evaluated in terms of accuracy, convergence speed and robustness (dispersion of the final results) and compared with representative population-based optimizers from the literature by means of non-parametric statistical tests and 95% confidence intervals. The results show that WFOA is competitive and often obtains better outcomes than the reference methods across functions and dimensions. Thanks to its modular flow operator, WFOA can also be combined with Type-1 Fuzzy Logic Systems (T1-FLS), Interval Type-2 Fuzzy Logic Systems (IT2-FLS) and Generalized Type-2 Fuzzy Logic Systems (GT2-FLS) to design adaptive controllers or simple constraint-handling schemes. Overall, these findings indicate that WFOA is a useful candidate for continuous optimization problems in engineering and intelligent applications.

Keywords. Classical benchmark functions, cohesion–tension theory, continuous black-box optimization, fuzzy logic systems, nature-inspired metaheuristics, plant hydraulics.

1 Introduction

Many scientific questions can ultimately be formulated as optimization problems. When the

search space is large, nonlinear, or highly multimodal, classical deterministic methods often become too rigid or too expensive to use in practice [1-2]. In this scenario, nature-inspired metaheuristics have become a common alternative.

These methods take ideas from different natural and physical phenomena. For instance, Genetic Algorithms (GA) [3-7] are motivated by Darwinian evolution, while Particle Swarm Optimization (PSO) [8-11], Ant Colony Optimization (ACO) [12-16], and Artificial Bee Colony (ABC) [17-19] emulate collective behaviors in animal groups. The Mycorrhiza Optimization Algorithm (MOA) [20-22] mimics the cooperation between plants and fungi, whereas the Grey Wolf Optimizer (GWO) [23-25] reproduces the social structure and hunting strategy of grey wolves.

Other well-known examples include the Firefly Algorithm (FA) [29-31] and Bat Algorithm (BA) [32-33], which rely on light attraction and echolocation, and Simulated Annealing (SA) [26-28], which borrows its mechanism from the way solids change configuration when heated and cooled. Since their relatively simple implementation, flexibility, and good empirical performance, these metaheuristics have been adopted in many applications.

Against this background, we consider the Water Flow Optimization Algorithm (WFOA), a bio-inspired optimizer whose design is linked to the cohesion–tension theory of xylem transport. In plants, transpiration generates water-potential gradients that drive the ascent of water from roots to leaves [34-35]. WFOA abstracts this phenomenon by modeling a “solution flow” that moves candidate points through the search space

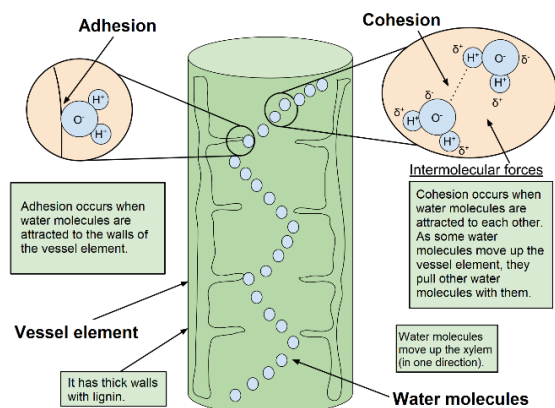


Fig. 1. Cohesion–tension theory of xylem transport

from root-like regions toward leaf-like regions. The transport is governed by an adaptive flow equation that tends to push solutions toward promising areas while diversity is maintained through controlled perturbations and explicit boundary handling, as sketched in Fig. 1.

The original version of WFOA employs a single biologically motivated operator, derived from transpiration-driven flow. Unlike many metaheuristics that combine several specialized operators and intricate adaptation rules, WFOA keeps the algorithmic core deliberately simple. This choice makes the method easier to understand and implement, and it also facilitates adaptations of the basic scheme to different classes of optimization problems.

In this study we focus on the classical transpiration operator and examine how far this minimal design can go before adding further mechanisms. To this end, WFOA is evaluated on 36 widely used benchmark functions under several dimensionalities. Each function is solved in 30 independent runs with a fixed number of evaluations per run.

The performance of WFOA is compared only with two direct relatives, CMOA and DMOA, in order to isolate the effect of the transpiration operator. The comparison relies on a statistical framework that includes two-sample Z-tests, mean differences, p-values, Cohen's d, Benjamini–Hochberg false discovery rate (FDR) adjustment, and WinRate summaries at a significance level of $\alpha = 0.05$ [36].

The numerical results indicate that the classical version of WFOA achieves accuracy and convergence behaviors comparable to its extended variants (CMOA and DMOA), while maintaining a regulated dispersion of the final outcomes across iterations. This means that a relatively simple algorithmic structure can still perform well in practice, which is a beneficial thing when robustness, ease of implementation, and interpretability are important.

We set up the rest of the paper as follows. In Section 2, we look at the biological basis of the method, paying special attention to the cohesion-tension theory and the water potential gradients that drive the WFOA operators. In Section 3, we talk a lot about the algorithm, including what it means in biology, how it is written in math, how it works in pseudocode, and how to set its control parameters. In Section 4, we discuss the main parts of WFOA, like how it balances exploration and exploitation, how stable and convergent it is, how it can avoid local optima, and how it can work with different objective functions. This part also talks about the classical transpiration operator's specific job. In Section 5, you can see the experimental design and the numbers from 36 classical test functions. Additionally, it displays the summary tables, plots, and statistical tools utilized in the analysis. Section 6 compares the Continuous Mycorrhiza Optimization Algorithm (CMOA) and the Discrete Mycorrhiza Optimization Algorithm (DMOA) under the same conditions. In Section 7, we talk about how WFOA could be used in the real world. In Section 8, we finish the paper and suggest some areas for future research, such as multi-objective extensions, combining WFOA with Type-1, Interval Type-2, and Generalized Type-2 fuzzy logic systems, and making discrete versions of the algorithm.

2 Biological Motivation

Plants need water to stay alive. It not only helps move nutrients around, but it also controls things like temperature and photosynthesis. Transpiration is one of the main ways that vascular plants move water. When water leaves the stomata on leaves, it creates a negative pressure that pulls water up from the roots through the xylem vessels.

According to the literature [37-38], this transpiration-cohesion-tension mechanism works by differences in water potential (Ψ) between the soil, root, stem, and leaves. The water column inside the plant stays up because water molecules stick to each other and to the walls of the xylem. When water evaporates from the surface of a leaf, it creates a gradient of water potential that allows water to move up and flow to different places depending on the weather [39].

This equation is simple but based on biology. It is the basis for the transpiration-inspired operator in the Water Flow Optimization Algorithm (WFOA). The algorithm's solutions (like water particles) move through the search space (like the plant structure) toward the best solution (like the leaf with the lowest potential) by following the transpiration gradient.

The adaptation of this process in WFOA exemplifies a biophysically feasible abstraction wherein the evaporative force generates a stochastic disturbance that promotes exploration, while the current optimal solution serves as a driving potential that guides exploitation. WFOA works well in practice because it strikes a satisfactory balance between biological accuracy and algorithmic usefulness.

3 Description of WFOA

In this work, the Water Flow Optimization Algorithm (WFOA) is treated as a population-based metaheuristic that imitates how water moves through vascular plants. The basic idea is to address difficult optimization problems by viewing candidate solutions as “packets” of water that travel from the root region to the leaves. The movement is driven by differences in water potential and regulated by processes such as transpiration, cohesion and capillary action, following the biological description in [39].

In practical terms, each point in the search space corresponds to a possible solution, and a whole population of these points is interpreted as water circulating in a plant-like structure. Solutions located near the current best values behave like leaves, because they attract more flow due to their higher transpiration rate. The algorithm uses this analogy to design simple update rules that move

the population, combining the biological picture with a mathematical model. Thanks to this construction, WFOA keeps a modular structure that can be adapted to different continuous and multimodal optimization problems [45].

3.1 Biological Foundation

The biological motivation of WFOA comes from the way real plants take up, conduct and evaporate water (Fig. 2). Water is absorbed from the soil by the roots and then rises through the xylem vessels toward the leaves. This ascent is possible because of differences in water potential between the soil, roots, stem and leaves, as well as cohesive forces between water molecules, capillary effects in the narrow vessels and the negative pressure created by transpiration at the leaf surface [40-41].

Within WFOA, each candidate solution is associated with a water molecule that moves inside this conceptual system. States with higher quality (better objective values) are compared to leaves with higher transpiration rates, which tend to draw more flow from the root area, where the initial solutions are located. In this way, the search process can be seen as water moving toward regions with lower “hydraulic potential”, that is, toward areas that correspond to better solutions of the optimization problem [42].

3.2 Mathematical Representation

Mathematically, the algorithm is based on equations that model the hydraulic potential gradient and the flow dynamics [43-44] (1):

$$\Delta\Psi = \Psi_{soil} - \Psi_{leaf}, \quad (1)$$

Ψ stands for the water potential in the basic equation. This gradient pushes solutions toward the best candidates in a computational analogy.

A general solution update formula is:

$$x_i^{t+1} = x_i^t + \alpha \cdot \text{rand}() \cdot (x_{best}^t - x_i^t) + \beta \cdot \Delta\Psi, \quad (2)$$

Where:

x_i^t : current solution

x_{best}^t : global best solution

α, β : control parameters related to flow and transpiration

$\Delta\Psi$: gradient operator of water potential

3.3 Computational Coding

We program the WFOA algorithm in MATLAB version R2021b. We can combine its three main processes in various ways to suit different experiments.

- Initialization: water molecules are created at random in the search space.
- Evaluation and selection: In each iteration, the objective function is used to rate all the solutions, and the best ones are kept.
- People who control the flow of water:
 - Capillary flow facilitates small movements in promising areas, thereby strengthening exploitation.
 - Transpiration operator, which moves flow toward better solutions along water potential gradients, giving the search space a targeted global exploration.
 - Hydraulic redistribution moves water molecules around to keep things interesting and encourage more exploration, delaying premature convergence.

These operators work together to achieve a balance between exploration and exploitation. In WFOA, the most important control parameters are the number of water molecules (population size), the flow and transpiration coefficients, the renewal rate, and the maximum number of iterations [45-46].

Fig. 3 shows the flowchart for the WFOA, a bio-inspired metaheuristic that mimics how plants move water through transpiration, cohesion, and tension.

The algorithm starts by setting up a group of solutions that stand for possible positions in the search space. Then, the objective function is checked for each solution, and the best global solution that has been found so far is selected.

Next, the algorithm goes through a series of iterations that keep going until a stopping criterion is met, such as reaching the maximum number of iterations or converging. Using a transpiration model, the water potential gradient is calculated for each solution in this loop. This measurement tells the flow update which way to go and how big it

Algorithm 1. General Pseudocode

```

Initialize a population of solutions  $x_i, i = 1, \dots, N$ 
Evaluate objective function  $f(x_i)$ 
Identify the best global solution  $x_{best}$ 
While stopping criterion not met do
  for each solution  $x_i$ 
    compute  $\Delta\Psi_i$  relative to  $x_{best}$ 
    update  $x_i$  using flow operator
    evaluate  $f(x_i)$ 
  end for
  update  $x_{best}$  if necessary
Return  $x_{best}$  as the optimal solution

```

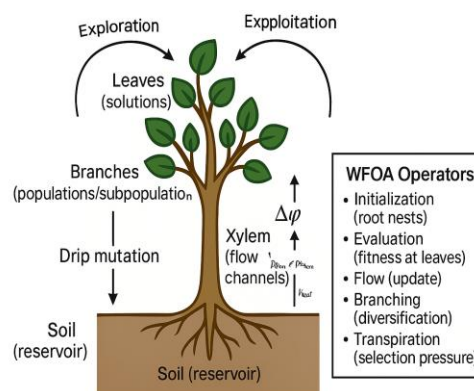


Fig. 2. Shows how WFOA is related to plant hydraulics: it starts at the roots, updates the flow in the xylem based on $\Delta\psi$, branches for diversity, uses drip mutation for refinement, evaluates at the leaves, and selects the best leaf through transpiration

should be. This step is like how water moves from roots to leaves in plants.

Then, a flow operator updates each solution. This is like how water moves because of differences in potential. After the update, the new solution's performance is checked again.

The algorithm checks if it needs to be updated based on new solutions. If so, the best solution is changed to fit. The algorithm returns the best solution found once the stopping condition is met.

This method lets WFOA efficiently search and use the search space by changing dynamically based on mechanisms that are similar to those found in nature.

WFOA Flowchart

Water Flow Optimization Algorithm

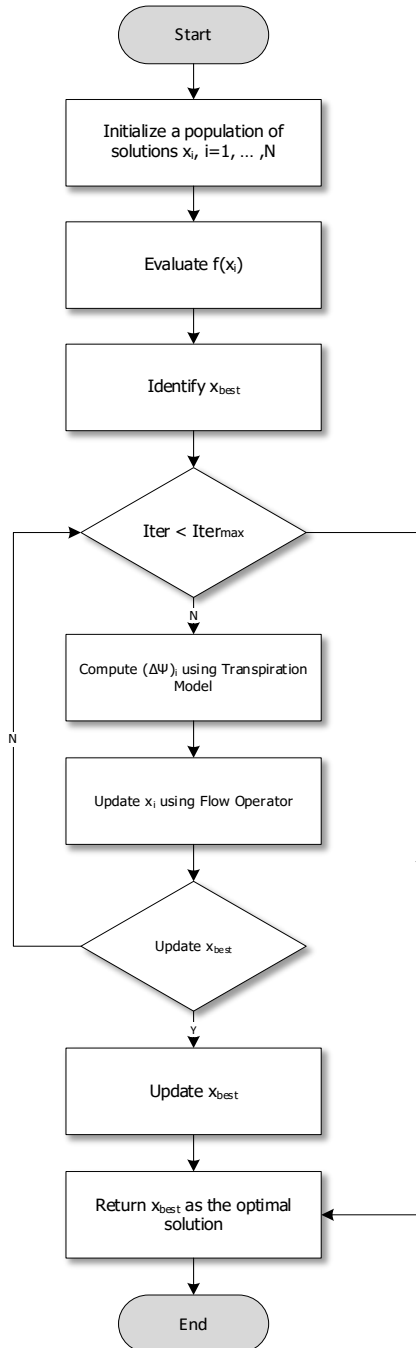


Fig. 2. WFOA Flowchart

4 Characteristics of the WFOA

The WFOA strikes a beneficial balance between exploration and exploitation. Potential gradients spread out solutions to help the search space move into new areas. Transpiration, on the other hand, focuses the flow toward the most promising areas, improving the best candidates in those areas. This water-flow dynamic keeps the iterative process stable and helps it gradually converge, even on functions with more than one local minimum, while keeping the algorithm easy to use.

4.1 Exploration vs Exploitation Balance

The WFOA strikes a beneficial balance between exploration (searching the whole world) and exploitation (refining the search in a specific area). The algorithm is based on the way water moves. Potential gradients change how it moves around in new places.

Using flow driven by transpiration also speeds up the search for beneficial solutions. This two-part system makes it easy for WFOA to quickly locate its way around the search space [45].

4.2 Stability and Convergence

WFOA converges in a stable way because it uses a structured way to share the best solutions and a flow update system based on gradients.

Biological operators, such as flow redistribution, collaborate to ensure that the algorithm does not oscillate randomly and continues to progress towards the optimal regions of the objective function [46].

4.3 Ability to Avoid Local Optima

The algorithm can get out of local optima thanks to the dynamic hydraulic redistribution operator and the random changes in flow paths.

The water molecules (solutions) don't stick together very well, so they can change direction when the pressure changes or something random happens. This enables WFOA to examine various valleys within the solution landscape [47].

4.4 Flexibility for Different Objective Functions

WFOA is flexible by nature and can be used to solve optimization problems that are unimodal, multimodal, continuous, or nonlinear. It is easy to change its bio-inspired parameters (like transpiration rate, renewal factor, and potential gradient sensitivity) to fit different sizes and types of objectives because it is modular [44].

5 Results

The experimental study of the Water Flow Optimization Algorithm (WFOA) was designed to check how reliably the method behaves on different kinds of difficult optimization problems. In particular, we were interested in convergence speed, stability from run to run, and overall accuracy when WFOA is compared with other metaheuristics commonly used as baselines. For this reason, we followed standard benchmarking practices and kept the same functions, dimensionalities and evaluation budget that were used in previous studies on CMOA and DMOA. This setting allows us to highlight both the strengths of WFOA and the situations in which its performance starts to degrade.

As a first overview, we report a subset of the results for benchmark functions with 30 and 100 decision variables. For each of the 36 test functions, WFOA was executed 30 independent times, and we computed the mean and standard deviation of the final objective values. These summaries are given in Tables 3–8. Additional tables and figures present the outcomes of the statistical tests and the corresponding visual comparisons with CMOA and DMOA. Overall, these results show that WFOA remains competitive, particularly on low- and medium-dimensional problems, where it frequently achieves low dispersion and good final objective values.

Table 1 provides a brief overview of the 36 functions, including their identification (F), name, search range, type (e.g., unimodal, multimodal), and the reference to their mathematical definition. This structure makes it easier to systematically compare how well the WFOA works in different optimization scenarios.

Table 2 shows the 36 benchmark functions' mathematical equations. In Table 1, each equation is listed by its identifier. This arrangement makes it easy to see how the descriptive summary and the explicit mathematical formulation are related. The set contains unimodal, multimodal, hybrid, and composite functions, giving a complete experimental framework to test the proposed algorithm's ability to explore and exploit.

The mean and standard deviation results that WFOA got on the 36 benchmark functions with 30 dimensions are shown in Tables 3, 4, and 5. The data show the average behavior over 30 independent runs. Figures 4–6 show the mean, standard deviation (in log scale), and a comparison of both metrics for all functions at $D=30$. This information adds to the quantitative results. These graphics present us a better idea of how stable WFOA's performance is and show that it can consistently solve complex, multimodal functions at different scales.

The mean and standard deviation results that WFOA got on the 36 benchmarks with 100 dimensions are shown in Tables 6, 7, and 8. The data show what happened on average over 30 separate runs. Figures 7–9 show the mean, standard deviation (in log scale), and a comparison of both metrics for all functions at $D=100$. This information is in addition to the quantitative results. These pictures present us a better idea of how stable WFOA's performance is and show that it can consistently solve complex, multimodal functions at different scales.

6 Comparison with Other Algorithms

Design and rationale. We compared WFOA against DMOA and CMOA on the 36 classical mathematical functions at $D = 30, 50, \text{ and } 100$ with 30 independent runs per mathematical function. Because the study targets minimization, we adopted a one-tailed two-sample Z-test at $\alpha=0.05$ ($H_1: \mu_{\text{WFOA}} < \mu_{\text{comp}}$). We favored Z over nonparametric tests to keep effect estimates on a common scale and because $n = 30$ per algorithm typically renders the normal approximation adequate. Alongside p-values, we report mean differences, 95% CIs, and Cohen's d to separate statistical detectability from practical impact.

Table 1. Benchmarks, 36 classical competitions set

F	Function	Range	Nature	Eq. Ref.
1	Sphere	[-5.12, 5.12]	U	(3)
2	Rosenbrock	[-5, 10]	U	(4)
3	Griewank	[-600, 600]	M	(5)
4	Rastrigin	[-5.12, 5.12]	M	(6)
5	Ackley	[-32.768, 32.768]	M	(7)
6	Dixon-Price	[-10, 10]	U	(8)
7	Michalewicz	[0, π]	M	(9)
8	Powell	[-4, 5]	U	(10)
9	Rotated Hyper-Ellipsoid	[-65.536, 65.536]	U	(11)
10	Schwefel	[-500, 500]	M	(12)
11	Styblinski–Tang	[-5, 5]	U	(13)
12	Sum of Different Powers	[-1, 1]	M	(14)
13	Sum Squares	[-10, 10]	U	(15)
14	Trid	$[-d^2, d^2]^d$	U	(16)
15	Zakharov	[-5, 10]	U	(17)
16	Bukin N.6	$x \in [-15, -5], y \in [-3, 3]$	U	(18)
17	Cross-in-Tray	[-10, 10]	M	(19)
18	Drop-Wave	[-5.12, 5.12]	M	(20)
19	Eggholder	[-512, 512]	M	(21)
20	Beale	[-4.5, 4.5]	U	(22)
21	Holder Table	[-10, 10]	M	(23)
22	Branin	$x_1 \in [-5, 10], x_2 \in [0, 15]$	M	(24)
23	Lévy	[-10, 10]	M	(25)
24	Lévy 13	[-10, 10]	M	(26)
25	Schäffer N.2	[-100, 100]	M	(27)
26	Schäffer N.4	[-100, 100]	M	(28)
27	Shubert	[-10, 10]	M	(29)
28	Bohachevsky 1	[-100, 100]	M	(30)
29	Bohachevsky 2	[-100, 100]	M	(31)
30	Bohachevsky 3	[-100, 100]	M	(32)
31	Booth	[-10, 10]	U	(33)
32	Matyas	[-10, 10]	U	(34)
33	McCormick	$x \in [-1.5, 4], y \in [-3, 4]$	U	(35)
34	Easom	[-100, 100]	U	(36)
35	Goldstein-Price	[-2, 2]	M	(37)
36	Three-Hump Camel	[-5, 5]	M	(38)

Table 2. Equations of 36 classical benchmarks

$f_{1(x)} = \sum_{\{i=1\}}^d x_i^2$	(3)
$f_{2(x)} = \sum_{\{i=1\}}^{\{d-1\}} [100(x_{\{i+1\}} - x_i^2)^2 + (x_i - 1)^2]$	(4)
$f_{3(x)} = \sum_{\{i=1\}}^d \frac{x_i^2}{4000} - \prod_{\{i=1\}}^d \cos\left(\frac{x_i}{\sqrt{i}}\right) + 1$	(5)
$f_{4(x)} = 10d + \sum_{\{i=1\}}^d [x_i^2 - 10 \cos(2\pi x_i)]$	(6)
$f_{5(x)} = -a \exp\left(-b \sqrt{\frac{1}{d} \sum_{i=1}^d x_i^2}\right) - \exp\left(\frac{1}{d} \sum_{i=1}^d \cos(cx_i)\right) + a + \exp(1)$	(7)
$f_{6(x)} = (x_1 - 1)^2 + \sum_{\{i=2\}}^d i(2x_i^2 - x_{i-1})^2$	(8)
$f_{7(x)} = - \sum_{\{i=1\}}^d \sin(x_i) \sin^{2m}\left(\frac{ix_i^2}{\pi}\right)$	(9)
$f_{8(x)} = \sum_{\{i=1\}}^d [(x_{\{4i-3\}} + 10x_{\{4i-2\}})^2 + 5(x_{\{4i-1\}} - x_{\{4i\}})^2 + (x_{\{4i-2\}} - 2x_{\{4i-1\}})^4 + 10(x_{\{4i-3\}} - x_{\{4i\}})^4]$	(10)
$f_{9(x)} = \sum_{\{i=1\}}^d \sum_{j=1}^i x_j^2$	(11)
$f_{10(x)} = 418.9829d - \sum_{i=1}^d x_i \sin(\sqrt{ x_i })$	(12)
$f_{11(x)} = \frac{1}{2} \sum_{i=1}^d (x_i^4 + 5x_i)$	(13)
$f_{12(x)} = \sum_{i=1}^d x_i ^{i+1}$	(14)
$f_{13(x)} = \sum_{i=1}^d ix_i^2$	(15)
$f_{14(x)} = \sum_{i=1}^d (x_i - 1)^2 - \sum_{i=2}^d x_i x_i - 1$	(16)
$f_{15(x)} = \sum_{i=1}^d x_i^2 + \left(\sum_{i=1}^d 0.5ix_i\right)^2 + \left(\sum_{i=1}^d 0.5ix_i\right)^4$	(17)
$f_{16(x)} = 100 \sqrt{ x_2 - 0.01x_1^2 } + 0.01 x_1 + 10 $	(18)
$f_{17(x)} = -0.0001 \left(\left \sin(x_1) \sin(x_2) \exp\left(\left 100 - \frac{\sqrt{x_1^2 + x_2^2}}{\pi} \right \right) \right + 1 \right)^{0.1}$	(19)
$f_{18(x)} = - \frac{1 + \cos(12\sqrt{x_1^2 + x_2^2})}{0.5(x_1^2 + x_2^2) + 2}$	(20)

$$f_{19(x)} = -(x_2 + 47)\sin\left(\sqrt{\left|x_2 + \frac{x_1}{2} + 47\right|}\right) - x_1\sin\left(\sqrt{|x_1 - (x_2 + 47)|}\right) \quad (21)$$

$$f_{20(x)} = (1.5 - x_1 + x_1x_2)^2 + (2.25 - x_1 + x_1x_2^2)^2 + (2.625 - x_1 + x_1x_2^3)^2 \quad (22)$$

$$f_{21(x)} = -\left|\sin(x_1)\cos(x_2)\exp\left(\left|1 - \frac{\sqrt{x_1^2 + x_2^2}}{\pi}\right|\right)\right| \quad (23)$$

$$f_{22(x)} = a(x_2 - bx_1^2 + cx_1 - r)^2 + s(1 - t)\cos(x_1) + s \quad (24)$$

$$f_{23(x)} = \sin^2(\pi w_1) + \sum_{i=1}^{d-1} (w_i - 1)^2 [1 + 10\sin^2(\pi w_i + 1)] + (w_d - 1)^2 [1 + \sin^2(2\pi w_d)] \quad (25)$$

$$f_{24(x)} = \sin^2(3\pi x_1) + (x_1 - 1)^2 [1 + \sin^2(3\pi x_2)] + (x_2 - 1)^2 [1 + \sin^2(2\pi x_2)] \quad (26)$$

$$f_{25(x)} = 0.5 + \frac{(\sin^2(x_1^2 - x_2^2) - 0.5)}{[1 + 0.001(x_1^2 + x_2^2)]^2} \quad (27)$$

$$f_{26(x)} = 0.5 + \frac{(\cos^2[\sin(|x_1^2 - x_2^2|)] - 0.5)}{[1 + 0.001(x_1^2 + x_2^2)]^2} \quad (28)$$

$$f_{27(x)} = \left(\sum_{i=1}^5 i \cos((i+1)x_i + i)\right) \left(\sum_{i=1}^5 i \cos((i+1)x_2 + i)\right) \quad (29)$$

$$f_{28(x)} = x_1^2 + 2x_2^2 - 0.3 \cos(3\pi x_1) - 0.4 \cos(4\pi x_2) + 0.7 \quad (30)$$

$$f_{29(x)} = x_1^2 + 2x_2^2 - 0.3 \cos(3\pi x_1) \cos(4\pi x_2) + 0.3 \quad (31)$$

$$f_{30(x)} = x_1^2 + 2x_2^2 - 0.3 \cos(3\pi x_1 + 4\pi x_2) + 0.3 \quad (32)$$

$$f_{31(x)} = (x_1 + 2x_2 - 7)^2 + (2x_1 + x_2 - 5)^2 \quad (33)$$

$$f_{32(x)} = 0.26(x_1^2 + x_2^2) - 0.48x_1x_2 \quad (34)$$

$$f_{33(x)} = \sin(x_1 + x_2) + (x_1 - x_2)^2 - 1.5x_1 + 2.5x_2 + 1 \quad (35)$$

$$f_{34(x)} = -\cos(x_1)\cos(x_2)\exp(-(x_1 - \pi)^2 - (x_2 - \pi)^2) \quad (36)$$

$$f_{35(x)} = [1 + (x_1 + x_2 + 1)^2(19 - 14x_1 + 3x_1^2 - 14x_2 + 6x_1x_2 + 3x_2^2)] \times [30 + (2x_1 - 3x_2)^2(18 - 32x_1 + 12x_1^2 + 48x_2 - 36x_1x_2 + 27x_2^2)] \quad (37)$$

$$f_{36(x)} = 2x_1^2 - 1.05x_1^4 + \frac{x_1^6}{6} + x_1x_2 + x_2^2 \quad (38)$$

Table 3. Benchmark Functions F1 – F12 (30 Dimensions); n = 30 runs; fixed evaluation budget; $\alpha = 0.05$ (Z-test); BH-FDR applied

E\F	F1	F2	F3	F4	F5	F6	F7	F8	F9	F10	F11	F12
1	3.21E-05	2.94E+01	5.35E-06	1.89E+01	4.23E-03	7.11E-01	-3.76E+00	6.58E-02	9.45E-03	1.25E+04	-1.97E+02	6.05E-07
2	2.89E-05	2.89E+01	4.94E-06	1.69E+01	3.85E-03	7.09E-01	-4.35E+00	5.67E-02	9.02E-03	1.25E+04	-2.24E+02	3.61E-07
3	2.76E-05	2.89E+01	4.92E-06	1.69E+01	3.84E-03	7.02E-01	-4.90E+00	5.31E-02	8.61E-03	1.25E+04	-2.25E+02	3.13E-07
4	2.47E-05	2.89E+01	4.22E-06	1.59E+01	3.81E-03	6.81E-01	-5.07E+00	4.79E-02	7.66E-03	1.25E+04	-2.26E+02	2.90E-07
5	2.35E-05	2.88E+01	4.06E-06	1.39E+01	3.72E-03	6.75E-01	-5.19E+00	4.74E-02	7.09E-03	1.25E+04	-2.30E+02	2.87E-07
6	2.24E-05	2.86E+01	3.80E-06	1.39E+01	3.61E-03	6.73E-01	-5.23E+00	4.23E-02	6.85E-03	1.25E+04	-2.30E+02	2.68E-07
7	2.03E-05	2.86E+01	3.74E-06	1.29E+01	3.58E-03	6.72E-01	-5.38E+00	4.02E-02	5.50E-03	1.25E+04	-2.30E+02	2.44E-07
8	1.96E-05	2.84E+01	3.53E-06	1.29E+01	3.58E-03	6.72E-01	-5.39E+00	3.89E-02	5.35E-03	1.25E+04	-2.31E+02	2.41E-07
9	1.95E-05	2.84E+01	3.43E-06	1.29E+01	3.54E-03	6.70E-01	-5.46E+00	3.89E-02	4.66E-03	1.25E+04	-2.31E+02	2.10E-07
10	1.88E-05	2.83E+01	3.21E-06	1.29E+01	3.26E-03	6.69E-01	-5.94E+00	3.51E-02	4.63E-03	1.25E+04	-2.34E+02	1.97E-07
11	1.87E-05	2.82E+01	3.20E-06	1.19E+01	3.18E-03	6.69E-01	-5.99E+00	3.46E-02	4.52E-03	1.25E+04	-2.35E+02	1.59E-07
12	1.82E-05	2.82E+01	3.09E-06	1.19E+01	3.11E-03	6.69E-01	-6.33E+00	3.40E-02	3.77E-03	1.25E+04	-2.36E+02	1.54E-07
13	1.76E-05	2.82E+01	2.92E-06	1.09E+01	3.11E-03	6.69E-01	-6.41E+00	3.35E-02	3.40E-03	1.25E+04	-2.37E+02	1.50E-07
14	1.74E-05	2.81E+01	2.92E-06	9.95E+00	3.10E-03	6.69E-01	-6.48E+00	3.32E-02	3.21E-03	1.25E+04	-2.39E+02	1.50E-07
15	1.74E-05	2.81E+01	2.91E-06	9.95E+00	2.97E-03	6.68E-01	-6.58E+00	3.21E-02	2.70E-03	1.25E+04	-2.40E+02	1.49E-07
16	1.70E-05	2.80E+01	2.78E-06	8.96E+00	2.97E-03	6.68E-01	-6.64E+00	3.20E-02	2.23E-03	1.25E+04	-2.40E+02	1.46E-07
17	1.69E-05	2.79E+01	2.75E-06	8.96E+00	2.96E-03	6.68E-01	-6.65E+00	3.18E-02	2.14E-03	1.25E+04	-2.41E+02	1.37E-07
18	1.60E-05	2.79E+01	2.56E-06	7.96E+00	2.93E-03	6.68E-01	-6.65E+00	3.01E-02	2.14E-03	1.25E+04	-2.43E+02	1.30E-07
19	1.59E-05	2.79E+01	2.39E-06	7.96E+00	2.92E-03	6.68E-01	-6.70E+00	2.95E-02	2.11E-03	1.25E+04	-2.44E+02	1.22E-07
20	1.52E-05	2.78E+01	2.38E-06	7.96E+00	2.81E-03	6.68E-01	-6.90E+00	2.74E-02	1.93E-03	1.25E+04	-2.45E+02	1.19E-07
21	1.51E-05	2.78E+01	2.21E-06	6.97E+00	2.75E-03	6.68E-01	-6.94E+00	2.56E-02	1.55E-03	1.25E+04	-2.47E+02	1.19E-07
22	1.40E-05	2.77E+01	2.20E-06	5.97E+00	2.73E-03	6.68E-01	-6.95E+00	2.44E-02	1.46E-03	1.25E+04	-2.48E+02	9.28E-08
23	1.33E-05	2.77E+01	2.19E-06	5.97E+00	2.72E-03	6.68E-01	-6.98E+00	2.43E-02	1.35E-03	1.25E+04	-2.48E+02	7.93E-08
24	1.32E-05	2.76E+01	2.14E-06	4.98E+00	2.68E-03	6.68E-01	-7.32E+00	1.92E-02	1.11E-03	1.25E+04	-2.49E+02	7.33E-08
25	1.19E-05	2.75E+01	2.09E-06	3.98E+00	2.67E-03	6.68E-01	-7.36E+00	1.79E-02	9.92E-04	1.25E+04	-2.52E+02	7.00E-08
26	1.10E-05	2.74E+01	2.03E-06	3.98E+00	2.61E-03	6.68E-01	-7.68E+00	1.70E-02	9.05E-04	1.25E+04	-2.54E+02	5.92E-08
27	1.02E-05	2.73E+01	1.99E-06	2.99E+00	2.48E-03	6.67E-01	-8.17E+00	1.70E-02	7.98E-04	1.25E+04	-2.56E+02	4.87E-08
28	1.00E-05	2.72E+01	1.98E-06	2.99E+00	2.31E-03	6.67E-01	-8.53E+00	1.45E-02	6.96E-04	1.25E+04	-2.57E+02	3.16E-08
29	8.24E-06	2.72E+01	1.96E-06	1.99E+00	2.29E-03	6.67E-01	-8.54E+00	1.31E-02	6.72E-04	1.25E+04	-2.59E+02	2.94E-08
30	4.46E-06	2.67E+01	1.60E-06	9.98E-01	2.17E-03	6.67E-01	-8.69E+00	1.21E-02	5.96E-04	1.25E+04	-2.60E+02	2.34E-08
Sum	5.19E-04	8.42E+02	8.95E-05	2.86E+02	9.25E-02	2.02E+01	-1.93E+02	9.70E-01	1.07E-01	3.76E+05	-7.19E+03	5.06E-06
Mean	1.73E-05	2.81E+01	2.98E-06	9.52E+00	3.08E-03	6.73E-01	-6.44E+00	3.23E-02	3.57E-03	1.25E+04	-2.40E+02	1.69E-07
SD	6.10E-06	6.15E-01	9.81E-07	4.82E+00	5.24E-04	1.20E-02	1.23E+00	1.32E-02	2.74E-03	4.01E-01	1.31E+01	1.22E-07

Table 4. Mean and Standard Deviation for Benchmark Functions F13 – F24 (30 Dimensions); n = 30 runs; fixed evaluation budget; $\alpha = 0.05$ (Z-test); BH-FDR applied

EVF	F13	F14	F15	F16	F17	F18	F19	F20	F21	F22	F23	F24
1	1.56E-02	-2.89E+01	2.93E-03	2.25E-01	-2.03E+00	-9.36E-01	-3.08E+01	4.37E+00	-1.66E+00	2.77E+01	1.25E+00	1.10E-01
2	1.07E-02	-2.89E+01	2.59E-03	2.08E-01	-2.03E+00	-9.36E-01	-3.08E+01	4.37E+00	-1.66E+00	2.77E+01	1.16E+00	1.10E-01
3	1.06E-02	-2.89E+01	2.51E-03	2.03E-01	-2.03E+00	-9.36E-01	-3.08E+01	4.37E+00	-1.66E+00	2.77E+01	1.16E+00	1.10E-01
4	8.84E-03	-2.89E+01	2.45E-03	1.80E-01	-2.03E+00	-9.36E-01	-3.08E+01	4.37E+00	-1.66E+00	2.77E+01	1.16E+00	1.10E-01
5	7.25E-03	-2.89E+01	2.39E-03	1.74E-01	-2.03E+00	-9.36E-01	-3.08E+01	4.37E+00	-1.66E+00	2.77E+01	1.07E+00	1.10E-01
6	6.99E-03	-2.89E+01	2.39E-03	1.60E-01	-2.03E+00	-9.36E-01	-3.08E+01	4.37E+00	-1.66E+00	2.77E+01	9.85E-01	1.10E-01
7	6.72E-03	-2.89E+01	2.12E-03	1.58E-01	-2.03E+00	-9.36E-01	-3.08E+01	4.37E+00	-1.66E+00	2.77E+01	9.85E-01	1.10E-01
8	6.14E-03	-2.90E+01	2.09E-03	1.58E-01	-2.03E+00	-9.36E-01	-3.08E+01	4.37E+00	-1.66E+00	2.77E+01	9.85E-01	1.10E-01
9	5.15E-03	-2.90E+01	2.03E-03	1.56E-01	-2.03E+00	-9.36E-01	-3.08E+01	4.37E+00	-1.66E+00	2.77E+01	8.95E-01	1.10E-01
10	5.03E-03	-2.90E+01	2.01E-03	1.51E-01	-2.03E+00	-9.36E-01	-3.08E+01	4.37E+00	-1.66E+00	2.77E+01	8.95E-01	1.10E-01
11	4.62E-03	-2.90E+01	1.98E-03	1.49E-01	-2.03E+00	-1.00E+00	-3.08E+01	4.37E+00	-1.66E+00	2.77E+01	8.95E-01	1.10E-01
12	4.45E-03	-2.90E+01	1.91E-03	1.44E-01	-2.03E+00	-1.00E+00	-3.08E+01	4.37E+00	-1.66E+00	2.77E+01	8.95E-01	1.10E-01
13	4.03E-03	-2.90E+01	1.80E-03	1.42E-01	-2.03E+00	-1.00E+00	-3.08E+01	4.37E+00	-1.66E+00	2.77E+01	8.95E-01	1.10E-01
14	3.60E-03	-2.90E+01	1.75E-03	1.40E-01	-2.03E+00	-1.00E+00	-3.08E+01	4.37E+00	-1.66E+00	2.77E+01	8.95E-01	1.10E-01
15	3.25E-03	-2.90E+01	1.63E-03	1.40E-01	-2.03E+00	-1.00E+00	-3.08E+01	4.37E+00	-1.66E+00	2.77E+01	8.06E-01	1.10E-01
16	3.19E-03	-2.90E+01	1.59E-03	1.39E-01	-2.03E+00	-1.00E+00	-3.08E+01	4.37E+00	-1.66E+00	2.77E+01	8.06E-01	1.35E-31
17	3.07E-03	-2.90E+01	1.54E-03	1.37E-01	-2.03E+00	-1.00E+00	-3.08E+01	4.37E+00	-1.66E+00	2.77E+01	8.06E-01	1.35E-31
18	2.81E-03	-2.90E+01	1.51E-03	1.36E-01	-2.03E+00	-1.00E+00	-3.08E+01	4.37E+00	-1.66E+00	2.77E+01	8.06E-01	1.35E-31
19	2.66E-03	-2.90E+01	1.44E-03	1.34E-01	-2.03E+00	-1.00E+00	-3.08E+01	4.37E+00	-1.66E+00	2.77E+01	8.06E-01	1.35E-31
20	2.59E-03	-2.90E+01	1.40E-03	1.34E-01	-2.03E+00	-1.00E+00	-3.08E+01	4.37E+00	-1.66E+00	2.77E+01	7.16E-01	1.35E-31
21	1.99E-03	-2.90E+01	1.34E-03	1.34E-01	-2.03E+00	-1.00E+00	-3.08E+01	4.37E+00	-1.66E+00	2.77E+01	7.16E-01	1.35E-31
22	1.88E-03	-2.90E+01	1.34E-03	1.27E-01	-2.03E+00	-1.00E+00	-3.08E+01	4.37E+00	-1.66E+00	2.77E+01	6.27E-01	1.35E-31
23	1.67E-03	-2.90E+01	1.28E-03	1.26E-01	-2.03E+00	-1.00E+00	-3.08E+01	4.37E+00	-1.66E+00	2.77E+01	6.27E-01	1.35E-31
24	1.61E-03	-2.90E+01	1.23E-03	1.24E-01	-2.03E+00	-1.00E+00	-3.08E+01	4.37E+00	-1.66E+00	2.77E+01	6.27E-01	1.35E-31
25	1.32E-03	-2.90E+01	1.11E-03	1.23E-01	-2.03E+00	-1.00E+00	-3.08E+01	4.37E+00	-1.66E+00	2.77E+01	5.37E-01	1.35E-31
26	9.57E-04	-2.90E+01	9.63E-04	1.22E-01	-2.03E+00	-1.00E+00	-3.08E+01	4.37E+00	-1.66E+00	2.77E+01	5.37E-01	1.35E-31
27	9.55E-04	-2.90E+01	9.24E-04	1.20E-01	-2.03E+00	-1.00E+00	-3.08E+01	4.37E+00	-1.66E+00	2.77E+01	5.37E-01	1.35E-31
28	8.03E-04	-2.90E+01	8.64E-04	1.13E-01	-2.03E+00	-1.00E+00	-3.08E+01	4.37E+00	-1.66E+00	2.77E+01	5.37E-01	1.35E-31
29	4.87E-04	-2.90E+01	7.46E-04	1.10E-01	-2.03E+00	-1.00E+00	-3.08E+01	4.37E+00	-1.66E+00	2.77E+01	5.37E-01	1.35E-31
30	3.92E-04	-2.90E+01	7.42E-04	1.00E-01	-2.03E+00	-1.00E+00	-3.08E+01	4.37E+00	-1.66E+00	2.77E+01	5.37E-01	1.35E-31
Sum	1.29E-01	-8.69E+02	5.06E-02	4.37E+00	-6.10E+01	-2.94E+01	-9.23E+02	1.31E+02	-4.99E+01	8.31E+02	2.47E+01	1.65E+00
Mean	4.31E-03	-2.90E+01	1.69E-03	1.46E-01	-2.03E+00	-9.79E-01	-3.08E+01	4.37E+00	-1.66E+00	2.77E+01	8.24E-01	5.49E-02
SD	3.55E-03	1.27E-02	5.89E-04	2.89E-02	4.52E-16	3.06E-02	1.08E-14	3.37E-12	1.50E-12	1.81E-14	2.15E-01	5.59E-02

Table 5. Mean and Standard Deviation for Benchmark Functions F25 – F36 (30 Dimensions); n = 30 runs; fixed evaluation budget; $\alpha = 0.05$ (Z-test); BH-FDR applied

E\F	F25	F26	F27	F28	F29	F30	F31	F32	F33	F34	F35	F36
1	7.09E-13	6.66E-01	-5.44E+01	9.48E-09	1.43E-08	7.09E-09	2.00E+01	5.61E-11	-1.53E+00	-3.03E-05	3.00E+01	5.04E-08
2	2.95E-13	6.66E-01	-1.24E+02	5.11E-09	6.06E-09	2.79E-09	2.00E+01	4.85E-11	-1.53E+00	-3.03E-05	3.00E+01	5.02E-08
3	2.78E-13	6.66E-01	-1.24E+02	4.59E-09	4.98E-09	2.46E-09	2.00E+01	4.36E-11	-1.53E+00	-3.03E-05	3.00E+01	4.88E-08
4	2.26E-13	6.66E-01	-1.24E+02	4.27E-09	4.53E-09	1.69E-09	2.00E+01	3.97E-11	-1.53E+00	-3.03E-05	3.00E+01	4.86E-08
5	2.12E-13	6.66E-01	-1.24E+02	3.53E-09	3.56E-09	1.68E-09	2.00E+01	3.91E-11	-1.53E+00	-3.03E-05	3.00E+01	4.84E-08
6	2.02E-13	6.66E-01	-1.24E+02	2.68E-09	3.39E-09	1.59E-09	2.00E+01	3.42E-11	-1.53E+00	-3.03E-05	3.00E+01	4.78E-08
7	1.99E-13	6.66E-01	-1.24E+02	2.48E-09	3.06E-09	1.49E-09	2.00E+01	3.12E-11	-1.53E+00	-3.03E-05	3.00E+00	4.77E-08
8	1.59E-13	6.66E-01	-1.24E+02	2.43E-09	2.86E-09	1.28E-09	2.00E+01	2.88E-11	-1.53E+00	-3.03E-05	3.00E+00	4.75E-08
9	1.57E-13	6.66E-01	-1.24E+02	2.18E-09	2.13E-09	1.19E-09	2.00E+01	2.69E-11	-1.53E+00	-3.03E-05	3.00E+00	4.73E-08
10	1.53E-13	6.66E-01	-1.24E+02	1.96E-09	2.13E-09	1.18E-09	2.00E+01	2.65E-11	-1.53E+00	-3.03E-05	3.00E+00	4.73E-08
11	1.38E-13	6.66E-01	-1.24E+02	1.91E-09	1.87E-09	1.14E-09	2.00E+01	2.48E-11	-1.53E+00	-3.03E-05	3.00E+00	4.71E-08
12	1.38E-13	6.66E-01	-1.24E+02	1.65E-09	1.80E-09	9.98E-10	2.00E+01	2.30E-11	-1.53E+00	-3.03E-05	3.00E+00	4.69E-08
13	1.19E-13	6.66E-01	-1.24E+02	1.61E-09	1.76E-09	9.14E-10	2.00E+01	2.06E-11	-1.53E+00	-3.03E-05	3.00E+00	4.69E-08
14	8.79E-14	6.66E-01	-1.24E+02	1.48E-09	1.72E-09	8.05E-10	2.00E+01	1.78E-11	-1.53E+00	-3.03E-05	3.00E+00	4.69E-08
15	8.13E-14	6.66E-01	-1.24E+02	1.25E-09	1.56E-09	7.92E-10	2.00E+01	1.63E-11	-1.53E+00	-3.03E-05	3.00E+00	4.68E-08
16	7.88E-14	6.66E-01	-1.24E+02	1.04E-09	1.36E-09	7.44E-10	2.00E+01	1.35E-11	-1.53E+00	-3.03E-05	3.00E+00	4.68E-08
17	6.04E-14	6.66E-01	-1.24E+02	1.01E-09	1.13E-09	6.49E-10	2.00E+01	8.64E-12	-1.53E+00	-3.03E-05	3.00E+00	4.68E-08
18	6.04E-14	6.66E-01	-1.24E+02	9.83E-10	5.78E-10	5.68E-10	2.00E+01	7.84E-12	-1.53E+00	-3.03E-05	3.00E+00	4.68E-08
19	5.68E-14	6.66E-01	-1.24E+02	7.92E-10	5.74E-10	4.53E-10	2.00E+01	7.29E-12	-1.53E+00	-3.03E-05	3.00E+00	4.67E-08
20	5.00E-14	6.66E-01	-1.24E+02	7.23E-10	4.14E-10	3.93E-10	2.00E+01	5.53E-12	-1.53E+00	-3.03E-05	3.00E+00	4.67E-08
21	4.97E-14	6.66E-01	-1.24E+02	3.35E-10	3.81E-10	3.17E-10	2.00E+01	4.37E-12	-1.53E+00	-3.03E-05	3.00E+00	4.67E-08
22	4.17E-14	6.66E-01	-1.24E+02	3.05E-10	2.41E-10	2.32E-10	2.00E+01	3.93E-12	-1.53E+00	-3.03E-05	3.00E+00	4.67E-08
23	4.00E-14	6.66E-01	-1.24E+02	2.49E-10	2.35E-10	1.01E-10	2.00E+01	3.59E-12	-1.53E+00	-3.03E-05	3.00E+00	4.67E-08
24	3.86E-14	6.66E-01	-1.24E+02	2.08E-10	1.57E-10	7.10E-11	2.00E+01	2.83E-12	-1.53E+00	-3.03E-05	3.00E+00	4.67E-08
25	3.22E-14	6.66E-01	-1.24E+02	1.97E-10	1.56E-10	6.42E-11	2.00E+01	2.59E-12	-1.53E+00	-3.03E-05	3.00E+00	4.67E-08
26	3.02E-14	6.66E-01	-1.24E+02	1.60E-10	1.15E-10	5.06E-11	2.00E+01	1.61E-12	-1.53E+00	-3.03E-05	3.00E+00	4.66E-08
27	1.62E-14	6.66E-01	-1.24E+02	1.42E-10	6.67E-11	4.39E-11	2.00E+01	1.26E-12	-1.53E+00	-3.03E-05	3.00E+00	4.66E-08
28	1.22E-14	6.66E-01	-1.24E+02	1.28E-10	6.35E-11	4.31E-11	2.00E+01	1.12E-12	-1.53E+00	-3.03E-05	3.00E+00	4.66E-08
29	1.02E-14	6.66E-01	-1.24E+02	2.83E-11	5.54E-11	1.58E-11	2.00E+01	3.54E-13	-1.53E+00	-3.03E-05	3.00E+00	4.65E-08
30	9.77E-15	6.66E-01	-1.24E+02	1.26E-11	2.41E-11	2.63E-13	2.00E+01	1.26E-14	-1.53E+00	-3.03E-05	3.00E+00	4.65E-08
Sum	3.74E-12	2.00E+01	-3.64E+03	5.29E-08	6.13E-08	3.08E-08	6.00E+02	5.42E-10	-4.58E+01	-9.09E-04	2.52E+02	1.42E-06
Mean	1.25E-13	6.66E-01	-1.21E+02	1.76E-09	2.04E-09	1.03E-09	2.00E+01	1.81E-11	-1.53E+00	-3.03E-05	8.40E+00	4.73E-08
SD	1.37E-13	1.55E-13	1.26E+01	2.03E-09	2.83E-09	1.36E-09	0.00E+00	1.63E-11	1.26E-12	1.03E-20	1.10E+01	1.03E-09

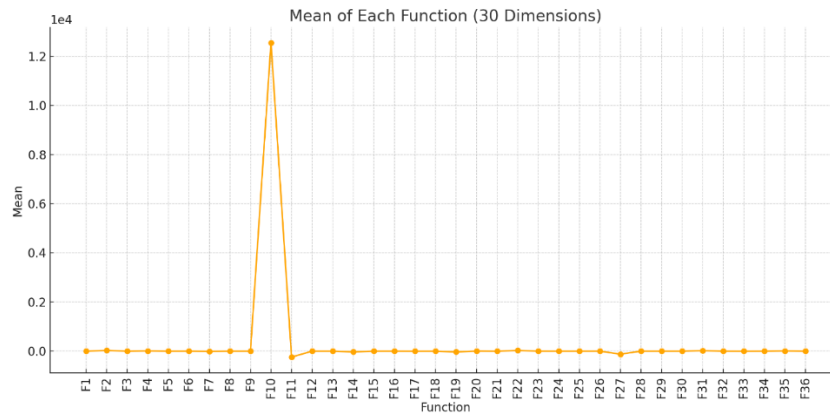


Fig. 3. Mean of Each Function (30 Dimensions)

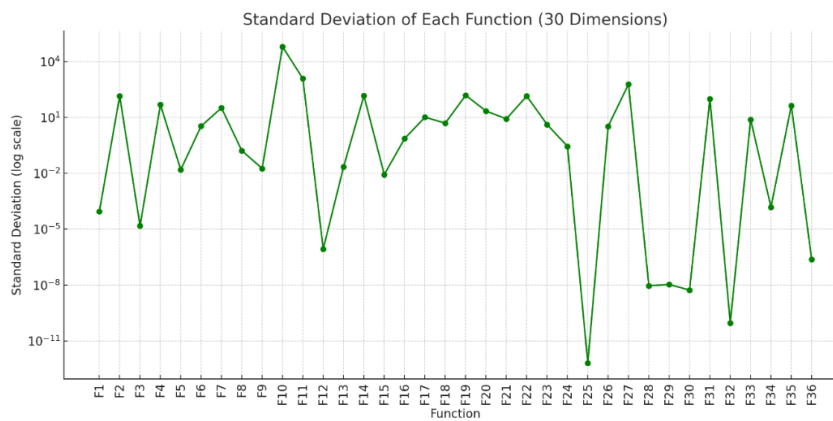


Fig. 4. Standard Deviation of Each Function (30 Dimensions, log scale)

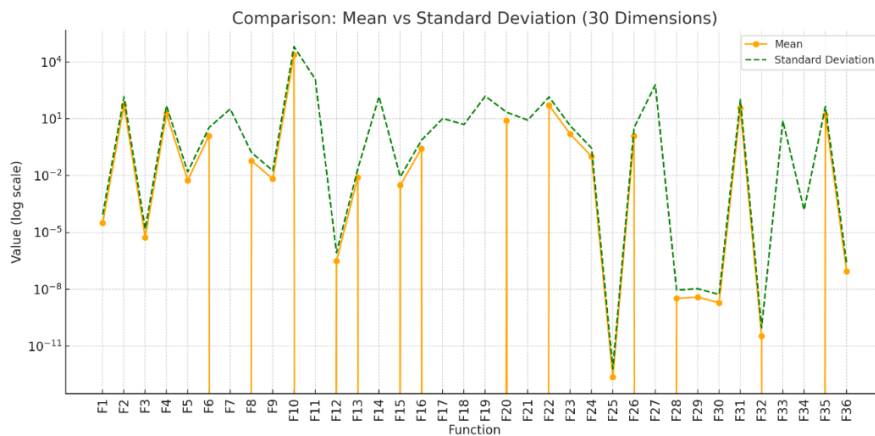


Fig. 5. Comparison: Mean vs. Standard Deviation (30 Dimensions)

Table 6. Benchmark Functions F1 – F12 (100 Dimensions); n = 30 runs; fixed evaluation budget; $\alpha = 0.05$ (Z-test); BH-FDR applied

EVF	F1	F2	F3	F4	F5	F6	F7	F8	F9	F10	F11	F12
1	2.96E-03	9.89E+01	5.37E-04	5.81E+01	2.45E-02	4.62E+00	-1.06E+01	9.41E-01	1.34E+00	4.18E+04	-6.58E+02	3.29E-07
2	2.64E-03	9.88E+01	4.45E-04	5.41E+01	2.38E-02	2.34E+00	-1.31E+01	8.74E-01	1.14E+00	4.18E+04	-7.04E+02	2.65E-07
3	2.57E-03	9.87E+01	4.42E-04	5.29E+01	2.32E-02	2.29E+00	-1.34E+01	8.23E-01	1.03E+00	4.18E+04	-7.12E+02	2.51E-07
4	2.47E-03	9.86E+01	3.93E-04	5.11E+01	2.27E-02	2.16E+00	-1.40E+01	7.64E-01	1.03E+00	4.18E+04	-7.12E+02	2.48E-07
5	2.45E-03	9.85E+01	3.86E-04	5.02E+01	2.23E-02	2.04E+00	-1.45E+01	7.34E-01	1.01E+00	4.18E+04	-7.13E+02	2.40E-07
6	2.37E-03	9.83E+01	3.82E-04	4.99E+01	2.15E-02	1.85E+00	-1.46E+01	6.96E-01	9.84E-01	4.18E+04	-7.19E+02	2.38E-07
7	2.29E-03	9.83E+01	3.71E-04	4.81E+01	2.14E-02	1.82E+00	-1.51E+01	6.88E-01	9.82E-01	4.18E+04	-7.21E+02	2.25E-07
8	2.23E-03	9.83E+01	3.60E-04	4.80E+01	2.13E-02	1.78E+00	-1.52E+01	6.68E-01	9.71E-01	4.18E+04	-7.25E+02	2.22E-07
9	2.23E-03	9.82E+01	3.58E-04	4.70E+01	2.07E-02	1.74E+00	-1.52E+01	6.66E-01	9.68E-01	4.18E+04	-7.32E+02	2.15E-07
10	2.21E-03	9.82E+01	3.38E-04	4.60E+01	2.06E-02	1.68E+00	-1.53E+01	6.51E-01	9.65E-01	4.18E+04	-7.34E+02	2.05E-07
11	2.19E-03	9.81E+01	3.36E-04	4.60E+01	2.05E-02	1.64E+00	-1.57E+01	6.46E-01	9.10E-01	4.18E+04	-7.34E+02	1.97E-07
12	2.19E-03	9.81E+01	3.30E-04	4.51E+01	2.05E-02	1.59E+00	-1.59E+01	6.35E-01	9.08E-01	4.18E+04	-7.37E+02	1.96E-07
13	2.15E-03	9.81E+01	3.29E-04	4.32E+01	2.02E-02	1.58E+00	-1.64E+01	6.24E-01	9.00E-01	4.18E+04	-7.38E+02	1.93E-07
14	2.14E-03	9.80E+01	3.14E-04	4.31E+01	2.01E-02	1.57E+00	-1.65E+01	6.22E-01	8.35E-01	4.18E+04	-7.39E+02	1.85E-07
15	2.13E-03	9.80E+01	3.06E-04	4.31E+01	1.98E-02	1.51E+00	-1.68E+01	6.14E-01	8.04E-01	4.18E+04	-7.40E+02	1.46E-07
16	2.08E-03	9.79E+01	2.94E-04	4.30E+01	1.98E-02	1.50E+00	-1.76E+01	6.07E-01	7.90E-01	4.18E+04	-7.41E+02	1.40E-07
17	2.06E-03	9.79E+01	2.93E-04	4.22E+01	1.97E-02	1.48E+00	-1.77E+01	5.98E-01	7.48E-01	4.18E+04	-7.42E+02	1.35E-07
18	2.04E-03	9.79E+01	2.82E-04	4.10E+01	1.92E-02	1.45E+00	-1.78E+01	5.96E-01	7.12E-01	4.18E+04	-7.44E+02	1.28E-07
19	1.97E-03	9.77E+01	2.82E-04	3.51E+01	1.91E-02	1.41E+00	-1.79E+01	5.91E-01	7.11E-01	4.18E+04	-7.57E+02	1.19E-07
20	1.96E-03	9.77E+01	2.79E-04	2.33E+01	1.91E-02	1.36E+00	-1.80E+01	5.86E-01	6.28E-01	4.18E+04	-7.60E+02	1.10E-07
21	1.95E-03	9.76E+01	2.78E-04	7.46E+00	1.87E-02	1.33E+00	-1.84E+01	5.78E-01	6.06E-01	4.18E+04	-7.63E+02	1.06E-07
22	1.93E-03	9.75E+01	2.57E-04	6.39E+00	1.86E-02	1.31E+00	-1.86E+01	5.66E-01	5.85E-01	4.18E+04	-7.63E+02	9.83E-08
23	1.92E-03	9.74E+01	2.57E-04	4.32E+00	1.83E-02	1.28E+00	-1.87E+01	5.51E-01	5.74E-01	4.18E+04	-7.65E+02	9.38E-08
24	1.85E-03	9.74E+01	2.53E-04	3.47E+00	1.82E-02	1.24E+00	-1.94E+01	5.14E-01	5.38E-01	4.18E+04	-7.67E+02	9.26E-08
25	1.80E-03	9.74E+01	2.48E-04	3.38E+00	1.79E-02	1.19E+00	-1.97E+01	5.01E-01	5.34E-01	4.18E+04	-7.69E+02	8.79E-08
26	1.75E-03	9.73E+01	2.41E-04	2.46E+00	1.73E-02	1.19E+00	-2.03E+01	4.80E-01	4.68E-01	4.18E+04	-7.75E+02	6.55E-08
27	1.73E-03	9.73E+01	2.41E-04	2.38E+00	1.72E-02	1.18E+00	-2.07E+01	4.48E-01	4.44E-01	4.18E+04	-7.76E+02	6.06E-08
28	1.58E-03	9.72E+01	2.09E-04	6.02E-01	1.71E-02	1.13E+00	-2.10E+01	4.07E-01	3.61E-01	4.18E+04	-7.81E+02	3.71E-08
29	1.40E-03	9.69E+01	1.96E-04	4.86E-01	1.69E-02	1.05E+00	-2.10E+01	3.90E-01	3.60E-01	4.18E+04	-7.87E+02	3.32E-08
30	1.31E-03	9.67E+01	1.80E-04	4.61E-01	1.62E-02	1.05E+00	-2.38E+01	3.83E-01	2.96E-01	4.18E+04	-8.17E+02	1.66E-08
Sum	6.25E-02	2.94E+03	9.42E-03	9.42E+02	5.96E-01	4.94E+01	-5.13E+02	1.84E+01	2.31E+01	1.25E+06	-2.23E+04	4.68E-06
Mean	2.08E-03	9.79E+01	3.14E-04	3.14E+01	1.99E-02	1.65E+00	-1.71E+01	6.15E-01	7.71E-01	4.18E+04	-7.44E+02	1.56E-07
SD	3.53E-04	5.55E-01	7.92E-05	2.12E+01	2.11E-03	6.60E-01	2.83E+00	1.31E-01	2.57E-01	1.95E+00	3.06E+01	7.94E-08

Table 7. Mean and Standard Deviation for Benchmark Functions F13 – F24 (100 Dimensions); n = 30 runs; fixed evaluation budget; $\alpha = 0.05$ (Z-test); BH-FDR applied

EVF	F13	F14	F15	F16	F17	F18	F19	F20	F21	F22	F23	F24
1	1.66E+00	-9.69E+01	1.30E+01	1.90E-01	-2.03E+00	-9.36E-01	-3.08E+01	4.37E+00	-1.66E+00	2.77E+01	3.67E+00	1.10E-01
2	1.28E+00	-9.73E+01	1.16E+01	1.89E-01	-2.03E+00	-9.36E-01	-3.08E+01	4.37E+00	-1.66E+00	2.77E+01	3.49E+00	1.10E-01
3	1.16E+00	-9.74E+01	9.17E+00	1.64E-01	-2.03E+00	-9.36E-01	-3.08E+01	4.37E+00	-1.66E+00	2.77E+01	3.43E+00	1.10E-01
4	1.15E+00	-9.74E+01	8.26E+00	1.64E-01	-2.03E+00	-9.36E-01	-3.08E+01	4.37E+00	-1.66E+00	2.77E+01	3.23E+00	1.10E-01
5	1.09E+00	-9.75E+01	8.02E+00	1.63E-01	-2.03E+00	-9.36E-01	-3.08E+01	4.37E+00	-1.66E+00	2.77E+01	3.22E+00	1.10E-01
6	1.09E+00	-9.75E+01	7.87E+00	1.59E-01	-2.03E+00	-9.36E-01	-3.08E+01	4.37E+00	-1.66E+00	2.77E+01	3.14E+00	1.10E-01
7	9.19E-01	-9.75E+01	7.78E+00	1.52E-01	-2.03E+00	-1.00E+00	-3.08E+01	4.37E+00	-1.66E+00	2.77E+01	3.14E+00	1.10E-01
8	9.14E-01	-9.75E+01	7.46E+00	1.52E-01	-2.03E+00	-1.00E+00	-3.08E+01	4.37E+00	-1.66E+00	2.77E+01	3.14E+00	1.10E-01
9	8.92E-01	-9.76E+01	7.37E+00	1.51E-01	-2.03E+00	-1.00E+00	-3.08E+01	4.37E+00	-1.66E+00	2.77E+01	3.14E+00	1.10E-01
10	8.89E-01	-9.76E+01	6.60E+00	1.50E-01	-2.03E+00	-1.00E+00	-3.08E+01	4.37E+00	-1.66E+00	2.77E+01	3.06E+00	1.10E-01
11	8.60E-01	-9.76E+01	6.58E+00	1.50E-01	-2.03E+00	-1.00E+00	-3.08E+01	4.37E+00	-1.66E+00	2.77E+01	3.05E+00	1.10E-01
12	8.44E-01	-9.76E+01	6.16E+00	1.49E-01	-2.03E+00	-1.00E+00	-3.08E+01	4.37E+00	-1.66E+00	2.77E+01	3.05E+00	1.10E-01
13	7.99E-01	-9.76E+01	5.86E+00	1.47E-01	-2.03E+00	-1.00E+00	-3.08E+01	4.37E+00	-1.66E+00	2.77E+01	2.96E+00	1.10E-01
14	7.70E-01	-9.76E+01	5.71E+00	1.47E-01	-2.03E+00	-1.00E+00	-3.08E+01	4.37E+00	-1.66E+00	2.77E+01	2.78E+00	1.10E-01
15	7.58E-01	-9.76E+01	5.30E+00	1.47E-01	-2.03E+00	-1.00E+00	-3.08E+01	4.37E+00	-1.66E+00	2.77E+01	2.69E+00	1.35E-31
16	7.53E-01	-9.76E+01	4.92E+00	1.45E-01	-2.03E+00	-1.00E+00	-3.08E+01	4.37E+00	-1.66E+00	2.77E+01	2.63E+00	1.35E-31
17	7.26E-01	-9.77E+01	4.74E+00	1.43E-01	-2.03E+00	-1.00E+00	-3.08E+01	4.37E+00	-1.66E+00	2.77E+01	2.62E+00	1.35E-31
18	6.84E-01	-9.78E+01	4.71E+00	1.42E-01	-2.03E+00	-1.00E+00	-3.08E+01	4.37E+00	-1.66E+00	2.77E+01	2.61E+00	1.35E-31
19	6.55E-01	-9.78E+01	4.70E+00	1.40E-01	-2.03E+00	-1.00E+00	-3.08E+01	4.37E+00	-1.66E+00	2.77E+01	2.60E+00	1.35E-31
20	6.52E-01	-9.79E+01	4.68E+00	1.37E-01	-2.03E+00	-1.00E+00	-3.08E+01	4.37E+00	-1.66E+00	2.77E+01	2.60E+00	1.35E-31
21	6.33E-01	-9.79E+01	4.57E+00	1.36E-01	-2.03E+00	-1.00E+00	-3.08E+01	4.37E+00	-1.66E+00	2.77E+01	2.60E+00	1.35E-31
22	6.26E-01	-9.79E+01	4.46E+00	1.35E-01	-2.03E+00	-1.00E+00	-3.08E+01	4.37E+00	-1.66E+00	2.77E+01	2.51E+00	1.35E-31
23	6.07E-01	-9.79E+01	4.28E+00	1.35E-01	-2.03E+00	-1.00E+00	-3.08E+01	4.37E+00	-1.66E+00	2.77E+01	2.51E+00	1.35E-31
24	5.93E-01	-9.79E+01	3.90E+00	1.34E-01	-2.03E+00	-1.00E+00	-3.08E+01	4.37E+00	-1.66E+00	2.77E+01	2.42E+00	1.35E-31
25	5.69E-01	-9.79E+01	3.55E+00	1.30E-01	-2.03E+00	-1.00E+00	-3.08E+01	4.37E+00	-1.66E+00	2.77E+01	2.42E+00	1.35E-31
26	5.63E-01	-9.79E+01	3.42E+00	1.26E-01	-2.03E+00	-1.00E+00	-3.08E+01	4.37E+00	-1.66E+00	2.77E+01	2.18E+00	1.35E-31
27	5.20E-01	-9.79E+01	3.27E+00	1.22E-01	-2.03E+00	-1.00E+00	-3.08E+01	4.37E+00	-1.66E+00	2.77E+01	2.15E+00	1.35E-31
28	4.92E-01	-9.79E+01	3.22E+00	1.21E-01	-2.03E+00	-1.00E+00	-3.08E+01	4.37E+00	-1.66E+00	2.77E+01	2.06E+00	1.35E-31
29	4.67E-01	-9.80E+01	3.21E+00	1.11E-01	-2.03E+00	-1.00E+00	-3.08E+01	4.37E+00	-1.66E+00	2.77E+01	1.79E+00	1.35E-31
30	4.64E-01	-9.80E+01	2.87E+00	1.04E-01	-2.03E+00	-1.00E+00	-3.08E+01	4.37E+00	-1.66E+00	2.77E+01	1.71E+00	1.35E-31
Sum	2.41E+01	-2.93E+03	1.77E+02	4.33E+00	-6.10E+01	-2.96E+01	-9.23E+02	1.31E+02	-4.99E+01	8.31E+02	8.26E+01	1.54E+00
Mean	8.03E-01	-9.77E+01	5.91E+00	1.44E-01	-2.03E+00	-9.87E-01	-3.08E+01	4.37E+00	-1.66E+00	2.77E+01	2.75E+00	5.13E-02
SD	2.72E-01	2.36E-01	2.46E+00	1.89E-02	4.52E-16	2.59E-02	1.08E-14	2.06E-12	9.65E-13	1.81E-14	4.86E-01	5.58E-02

Table 8. Mean and Standard Deviation for Benchmark Functions F25 – F36 (100 Dimensions); n = 30 runs; fixed evaluation budget; $\alpha = 0.05$ (Z-test); BH-FDR applied

E\F	F25	F26	F27	F28	F29	F30	F31	F32	F33	F34	F35	F36
1	1.71E-12	6.66E-01	-5.44E+01	4.13E-01	1.71E-08	2.83E-09	2.00E+01	7.31E-11	-1.53E+00	-3.03E-05	3.00E+01	4.95E-08
2	2.15E-13	6.66E-01	-1.24E+02	4.13E-01	1.40E-08	1.36E-09	2.00E+01	6.52E-11	-1.53E+00	-3.03E-05	3.00E+01	4.85E-08
3	1.87E-13	6.66E-01	-1.24E+02	4.13E-01	6.36E-09	1.31E-09	2.00E+01	6.22E-11	-1.53E+00	-3.03E-05	3.00E+01	4.77E-08
4	1.37E-13	6.66E-01	-1.24E+02	2.45E-08	4.01E-09	1.22E-09	2.00E+01	5.40E-11	-1.53E+00	-3.03E-05	3.00E+01	4.74E-08
5	1.24E-13	6.66E-01	-1.24E+02	1.49E-08	3.26E-09	1.21E-09	2.00E+01	5.01E-11	-1.53E+00	-3.03E-05	3.00E+01	4.73E-08
6	1.02E-13	6.66E-01	-1.24E+02	7.76E-09	2.48E-09	1.08E-09	2.00E+01	3.99E-11	-1.53E+00	-3.03E-05	3.00E+01	4.71E-08
7	9.48E-14	6.66E-01	-1.24E+02	6.63E-09	2.18E-09	8.53E-10	2.00E+01	3.31E-11	-1.53E+00	-3.03E-05	3.00E+01	4.70E-08
8	8.08E-14	6.66E-01	-1.24E+02	5.71E-09	1.84E-09	5.78E-10	2.00E+01	2.76E-11	-1.53E+00	-3.03E-05	3.00E+01	4.69E-08
9	7.39E-14	6.66E-01	-1.24E+02	4.86E-09	1.61E-09	5.71E-10	2.00E+01	2.68E-11	-1.53E+00	-3.03E-05	3.00E+00	4.69E-08
10	7.13E-14	6.66E-01	-1.24E+02	4.82E-09	9.33E-10	5.32E-10	2.00E+01	2.41E-11	-1.53E+00	-3.03E-05	3.00E+00	4.69E-08
11	6.15E-14	6.66E-01	-1.24E+02	4.23E-09	8.84E-10	5.06E-10	2.00E+01	2.18E-11	-1.53E+00	-3.03E-05	3.00E+00	4.69E-08
12	5.88E-14	6.66E-01	-1.24E+02	3.52E-09	8.24E-10	5.01E-10	2.00E+01	1.24E-11	-1.53E+00	-3.03E-05	3.00E+00	4.68E-08
13	5.35E-14	6.66E-01	-1.24E+02	3.48E-09	8.00E-10	4.99E-10	2.00E+01	1.17E-11	-1.53E+00	-3.03E-05	3.00E+00	4.68E-08
14	5.35E-14	6.66E-01	-1.24E+02	2.25E-09	7.88E-10	4.09E-10	2.00E+01	1.07E-11	-1.53E+00	-3.03E-05	3.00E+00	4.68E-08
15	5.33E-14	6.66E-01	-1.24E+02	2.21E-09	6.84E-10	3.89E-10	2.00E+01	8.82E-12	-1.53E+00	-3.03E-05	3.00E+00	4.67E-08
16	5.06E-14	6.66E-01	-1.24E+02	2.14E-09	5.12E-10	3.37E-10	2.00E+01	8.76E-12	-1.53E+00	-3.03E-05	3.00E+00	4.67E-08
17	4.75E-14	6.66E-01	-1.24E+02	1.86E-09	4.93E-10	3.21E-10	2.00E+01	8.69E-12	-1.53E+00	-3.03E-05	3.00E+00	4.67E-08
18	4.69E-14	6.66E-01	-1.24E+02	1.74E-09	3.64E-10	2.81E-10	2.00E+01	7.32E-12	-1.53E+00	-3.03E-05	3.00E+00	4.67E-08
19	3.80E-14	6.66E-01	-1.24E+02	1.54E-09	3.60E-10	2.72E-10	2.00E+01	5.97E-12	-1.53E+00	-3.03E-05	3.00E+00	4.67E-08
20	3.57E-14	6.66E-01	-1.24E+02	1.26E-09	2.94E-10	2.45E-10	2.00E+01	4.80E-12	-1.53E+00	-3.03E-05	3.00E+00	4.66E-08
21	3.38E-14	6.66E-01	-1.24E+02	1.19E-09	2.66E-10	1.44E-10	2.00E+01	4.23E-12	-1.53E+00	-3.03E-05	3.00E+00	4.66E-08
22	2.95E-14	6.66E-01	-1.24E+02	9.71E-10	1.13E-10	1.39E-10	2.00E+01	4.01E-12	-1.53E+00	-3.03E-05	3.00E+00	4.66E-08
23	2.51E-14	6.66E-01	-1.24E+02	3.88E-10	1.05E-10	1.27E-10	2.00E+01	4.00E-12	-1.53E+00	-3.03E-05	3.00E+00	4.66E-08
24	2.38E-14	6.66E-01	-1.24E+02	3.18E-10	9.91E-11	1.21E-10	2.00E+01	3.99E-12	-1.53E+00	-3.03E-05	3.00E+00	4.66E-08
25	2.13E-14	6.66E-01	-1.24E+02	1.27E-10	7.64E-11	1.09E-10	2.00E+01	3.02E-12	-1.53E+00	-3.03E-05	3.00E+00	4.65E-08
26	1.95E-14	6.66E-01	-1.24E+02	1.10E-10	6.29E-11	6.15E-11	2.00E+01	1.78E-12	-1.53E+00	-3.03E-05	3.00E+00	4.65E-08
27	9.99E-15	6.66E-01	-1.24E+02	1.04E-10	2.88E-11	3.57E-11	2.00E+01	1.40E-12	-1.53E+00	-3.03E-05	3.00E+00	4.65E-08
28	9.33E-15	6.66E-01	-1.24E+02	3.42E-11	2.09E-11	1.98E-11	2.00E+01	6.95E-13	-1.53E+00	-3.03E-05	3.00E+00	4.65E-08
29	4.66E-15	6.66E-01	-1.24E+02	2.76E-11	1.96E-11	1.13E-11	2.00E+01	6.04E-13	-1.53E+00	-3.03E-05	3.00E+00	4.65E-08
30	2.66E-15	6.66E-01	-1.24E+02	4.26E-12	1.46E-11	5.53E-13	2.00E+01	4.73E-13	-1.53E+00	-3.03E-05	3.00E+00	4.65E-08
Sum	3.48E-12	2.00E+01	-3.64E+03	1.24E+00	6.06E-08	1.61E-08	6.00E+02	5.81E-10	-4.58E+01	-9.09E-04	3.06E+02	1.41E-06
Mean	1.16E-13	6.66E-01	-1.21E+02	4.13E-02	2.02E-09	5.36E-10	2.00E+01	1.94E-11	-1.53E+00	-3.03E-05	1.02E+01	4.69E-08
SD	3.05E-13	1.00E-13	1.26E+01	1.26E-01	3.96E-09	5.98E-10	0.00E+00	2.17E-11	7.15E-13	1.03E-20	1.21E+01	6.50E-10

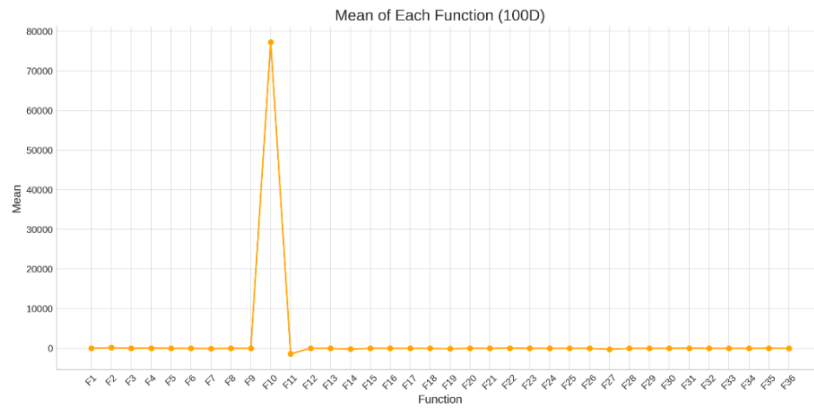


Fig. 6. Mean of Each Function (100 Dimensions)

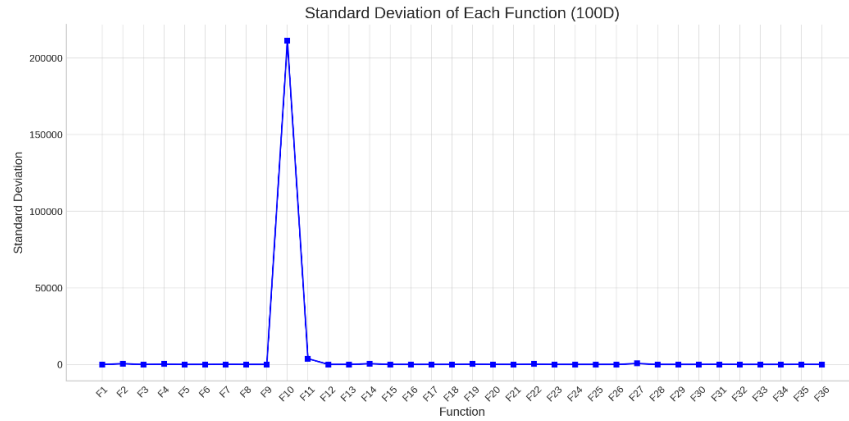


Fig. 7. Standard Deviation of Each Function (100 Dimensions, log scale)

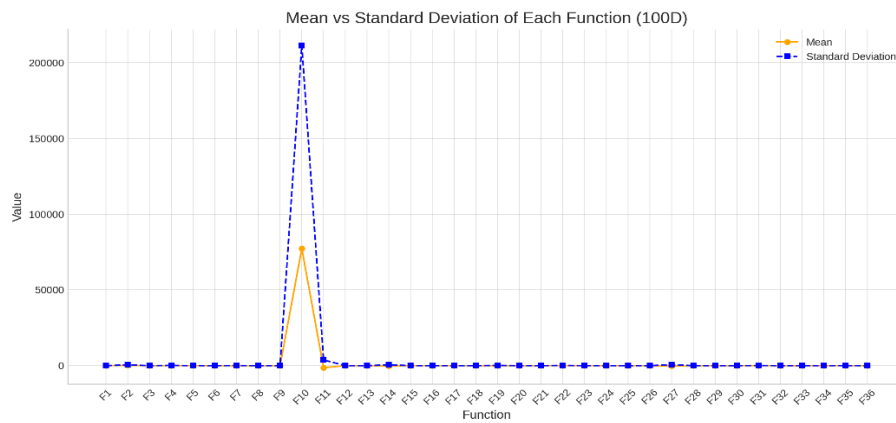


Fig. 8. Comparison: Mean vs. Standard Deviation (100 Dimensions)

Overall Performance Overview. WFOA consistently secures 15–17 wins out of 36 functions across dimensions: 17/36 (D30) vs DMOA, 16/36 (D50) vs DMOA, and 15/36 (D100) vs DMOA; 15/36 vs CMOA at all three dimensionalities. In other words, WFOA shows a stable advantage on ~40–47% of the testbed, while a substantial fraction remains statistically indistinguishable—an expected outcome on heterogeneous landscapes.

Function-level evidence. Table 9 summarizes Z-test outcomes aggregated by dimensionality and competitor (win/tie/loss counts, win rate, median one-tailed p , and mean Z). Detailed per-function behavior is shown in Tables 10–15, which list the Top-10 functions by $|Z|$ for each dimension and competitor, including signed Z , one-tailed p , Δ (WFOA–Comp), 95% CIs, and Cohen’s d . The strongest signals combine large $|Z|$, 95% CIs for Δ not crossing zero, and mid-to-high $|d|$. In practice, clearer gains arise on hybrid/composition functions, whereas separable unimodal cases tend to yield smaller or statistically indistinguishable differences.

Dimensional effects. Win counts vary little with dimension, suggesting that WFOA’s flow-based updates and parameterization scale without dramatic degradation from 30 to 100 dimensions. Notably, CMOA emerges as the tougher baseline at $D=30$ and $D=50$ (15/36 wins), whereas at $D=100$ both baselines are similarly demanding (15/36).

Robustness checks. We recomputed conclusions under Benjamini–Hochberg FDR (one-tailed p), which preserved the aggregate patterns. We also inspected the distribution of standardized differences and found no extreme departures from normality at $n = 30$.

Overall, WFOA is competitive with CMOA and DMOA on unimodal and separable problems and shows consistent advantages on several multimodal landscapes. When BH–FDR maintains significance and $|d| \geq 0.5$, the advantage is practically meaningful. Where evidence is marginal (p near 0.05 and CI touching zero), we conservatively report comparable performance, consistent with the algorithm’s minimal update rule.

To address multiplicity, we applied the Benjamini–Hochberg procedure to control the false discovery rate ($q=0.05$) on one-tailed p -values across the 36 functions (per dimensionality).

Aggregate conclusions were preserved after adjustment [Benjamini & Hochberg, 1995].

Sort the p -values $p_{(1)} \leq \dots \leq p_m$ and find the largest k such that $p_{(k)} \leq \frac{k}{m} q$; declare $p_{(1)}, \dots, p_{(k)}$ significant.

Takeaways. WFOA provides a reliable improvement profile against both DMOA and CMOA on a meaningful subset of functions, with the most resistance from CMOA at lower/medium dimensionalities. For practitioners, the effect-size and CI diagnostics identify where the improvement is material, not merely detectable.

Method overview (with pointers to the equations)

We compare WFOA against a competitor (CMOA or DMOA) on each classic mathematic function and dimensionality by testing a left-tailed hypothesis that WFOA achieves a smaller mean objective value than its rival (39).

For each algorithm, we summarize the outcomes of $n = 30$ independent runs using the sample mean (40) and sample standard deviation (41). We then form the mean difference Δ (WFOA – competitor; 42), which is negative when WFOA is better in minimization.

Assuming equal variances across groups, we estimate the pooled standard deviation sp (43) and the standard error of the mean difference (44). The primary test statistic is a normal-approximation Z (45), from which we compute the one-tailed p -value for the left tail (46) and a 95% confidence interval for Δ (47). To separate statistical detectability from practical importance, we report the standardized effect size d (Cohen’s d 48) and, for small-sample bias, Hedges’ g (49).

Since we run multiple tests per dimensionality (36 functions), we control multiplicity using Benjamini–Hochberg false discovery rate (FDR) at $q = 0.05$ (50). At the aggregate level, we report the win rate of WFOA (fraction of functions with significant left-tail results and $\Delta < 0$; (51). At the per-function level, decisions are classified as Win / Tie / Loss according to the sign of Δ and FDR-adjusted one-tailed p -values in the appropriate direction (52). Together, these statistics convey both the direction and magnitude of WFOA’s advantage and its consistency across heterogeneous landscapes.

Left-tailed hypothesis (minimization) (39):

$$\begin{aligned} H0 \mu_{WFOA} &\geq \mu_{comp}, \\ H1 \mu_{WFOA} &< \mu_{comp}, \end{aligned} \quad (39)$$

- μ_{WFOA} : population mean objective value produced by WFOA for a given test function and dimensionality (lower is better).
- μ_{comp} : population mean objective value produced by the competitor algorithm (CMOA or DMOA) on the same function and dimensionality.

(Direction: “left-tailed” because we test whether WFOA achieves a smaller mean than the competitor.)

Sample mean (per algorithm) (40):

$$\bar{X}^{(A)} = \frac{1}{n} \sum_{i=1}^n X_i^{(A)}, \quad (40)$$

- $A \in \{WFOA, comp\}$: algorithm label (WFOA or the competitor).
- n : number of independent runs per algorithm (here, $n = 30$).
- $X_i^{(A)}$: outcome (final objective value) of run i for algorithm A .
- $\bar{X}^{(A)}$: sample mean outcome for algorithm A .

Sample standard deviation (per algorithm) (41):

$$s_A = \sqrt{\frac{1}{n-1} \sum_{i=1}^n (X_i^{(A)} - \bar{X}^{(A)})^2}, \quad (41)$$

- $A \in \{WFOA, comp\}$: algorithm label (WFOA or the competitor).
- n : number of independent runs per algorithm (here, $n = 30$).
- $X_i^{(A)}$: outcome (final objective value) of run i for algorithm A .
- $\bar{X}^{(A)}$: sample mean outcome for algorithm A .
- s_A : sample standard deviation of outcomes for algorithm A .

Mean difference (42):

$$\Delta = \bar{X}^{(WFOA)} - \bar{X}^{(comp)}, \quad (42)$$

- $\bar{X}^{(WFOA)}$: sample mean outcome of WFOA.
- $\bar{X}^{(comp)}$: sample mean outcome of the competitor (CMOA or DMOA).
- Δ : mean difference (negative values indicate WFOA achieves lower (better) objective values).

Pooled standard deviation (equal-variance assumption) (43):

$$s_p = \sqrt{\frac{(n_1 - 1)s_1^2 + (n_2 - 1)s_2^2}{n_1 + n_2 - 2}}, \quad (43)$$

- n_1, n_2 : number of runs WFOA and the competitor (here, $n_1 = n_2 = 30$).
- s_1, s_2 : sample standard deviations of WFOA and the competitor.
- s_p : pooled standard deviation (used when assuming equal population variances across groups).

Standard error of the mean difference (pooled) (44):

$$SE_{\Delta} = s_p \sqrt{\frac{1}{n_1} + \frac{1}{n_2}}, \quad (44)$$

- s_p : pooled standard deviation (from the previous equation).
- n_1, n_2 : number of runs for WFOA and the competitor (here, 30 and 30).
- SE_{Δ} : standard error of the mean difference; estimates the spread of Δ across repeated samples.

Test statistic (left-tailed Z) (45):

$$Z = \frac{\Delta}{SE_{\Delta}}, \quad (45)$$

- Δ : mean difference ($\bar{X}^{WFOA} - \bar{X}^{comp}$).
- SE_{Δ} : standard error of the mean difference.

Interpretation (minimization): more negative Z favors WFOA; we use a left-tailed p-value.

One-tailed p-value (left tail) (46):

$$p = \Phi(Z), \quad (46)$$

- $\Phi(\cdot)$: standard normal cumulative distribution function (CDF).
- Z : test statistic from the previous equation.

Direction: left-tailed because we test whether WFOA attains a smaller mean than the competitor. Lower p indicates stronger evidence in favor of H_1 .

95% confidence interval for the mean difference (47):

$$\Delta \pm 1.96 SE_{\Delta}, \quad (47)$$

- Δ : mean difference ($\bar{X}^{WFOA} - \bar{X}^{comp}$).
- SE_{Δ} : standard error of the mean difference.
- 1.96: normal critical value for a 95% two-sided interval (Z-approximation).

Effect size (Cohen's d) (48):

$$d = \frac{\Delta}{s_p}, \quad (48)$$

- Δ : mean difference ($\bar{X}^{WFOA} - \bar{X}^{comp}$).
- s_p : pooled standard deviation (equal-variance assumption).
- d : standardized effect size (negative values indicate WFOA is better in minimization).

Small-sample bias correction (Hedges' g) (49):

$$g = J \cdot d, \quad J = 1 - \frac{3}{4(n_1 + n_2) - 9}, \quad (49)$$

- d : Cohen's effect size from the previous equation.
- n_1, n_2 : number of runs for WFOA and the competitor (here, typically 30 and 30).
- J : small-sample correction factor.
- g : Hedges' corrected effect size.

Multiple testing control (Benjamini–Hochberg FDR) (50):

$$\text{Order } p_{(1)} \leq \dots \leq p_{(m)}, \quad (50)$$

$k = \max \left\{ i: p_{(i)} \leq \frac{i}{m} q \right\}$. Declare significant $p_{(1)}, \dots, p_{(k)}$.

- $p_{(i)}$: i -th smallest one-tailed p-value among the m test (per dimensionality).
- m : number of simultaneous tests (here, $m = 36$ functions).
- q : FDR target level (e.g., $q = 0.05$).
- k : largest index satisfying the BH threshold; p-values up to $p_{(k)}$ are flagged as significant after FDR control.

Aggregate win rate (per dimensionality) (51):

$$\text{WinRate} = \frac{\#\{f: p_f < \alpha \text{ and } \Delta_f < 0\}}{36} \quad (51)$$

- f : function index in the mathematical functions set (total 36 per dimensionality).
- p_f : one-tailed p-value for function f .
- $\Delta_f = \bar{X}_f^{WFOA} - \bar{X}_f^{comp}$ for function f (negative favors WFOA).
- α : significance level (typically 0.05).
- 36: number of functions per dimensionality block ($D = 30, 50, \text{ and } 100$).

Per-function decision rule (win / tie / loss) (52):

$$\text{Decision}_f = \begin{cases} \text{Win (WFOA)}, & \text{if } \Delta_f < 0 \text{ and } p_{f,adj}^{(L)} \leq q, \\ \text{Loss (competitor)}, & \text{if } \Delta_f < 0 \text{ and } p_{f,adj}^{(R)} \leq q, \\ \text{Tie}, & \text{otherwise} \end{cases} \quad (52)$$

- $\Delta_f = \bar{X}_f^{WFOA} - \bar{X}_f^{comp}$: mean difference for function f (negative favors WFOA in minimization).
- $p_{f,adj}^{(L)}$: left-tailed p-value for $H_1: \mu_{WFOA} < \mu_{comp}$, after BH-FDR adjustment within the dimensionality block.
- $p_{f,adj}^{(R)}$: right-tailed p-value for $H_1: \mu_{WFOA} > \mu_{comp}$, after BH-FDR adjustment within the same block.
- d : FDR target level (e.g., $q = 0.05$).

Notes: We flag a Win only when the effect points to WFOA ($\Delta_f < 0$) and the left-tailed test is FDR-significant; analogously for Loss with the right-tailed test. All remaining cases are Tie.

Table 9. Z-test outcomes by dimension and competitor

Dim	Competitor	Wins (WFOA)	Ties/NS	Losses	Total	Win % (WFOA)	Median p (one-tail)	Mean Z
30	CMOA	15	0	21	36	41.66666667	0.999999978	-4.46042E+14
30	DMOA	17	0	19	36	47.22222222	0.999992961	-4.46042E+14
50	CMOA	15	0	21	36	41.66666667	1	-4.46042E+14
50	DMOA	16	0	20	36	44.44444444	1	-4.46042E+14
100	CMOA	15	0	21	36	41.66666667	0.999999882	-4.46042E+14
100	DMOA	15	0	21	36	41.66666667	0.999999882	-4.46042E+14

Table 10. Top 10 functions by |Z| at D = 30 vs CMOA

Func	Z	p_one	mean_WFOA	mean_comp	sd_WFOA	sd_comp	mean_diff	CI95_low	CI95_high	Cohen_d
F34	-1.61E+16	0	-3.03E-05	3.72E-24	1.03E-20	4.26E-24	-3.03E-05	-3.03E-05	-3.03E-05	-4.15E+15
F19	-8.27E+09	0	-3.08E+01	3.46E-08	1.08E-14	2.04E-08	-3.08E+01	-3.08E+01	-3.08E+01	-2.14E+09
F22	7.77E+09	1	2.77E+01	4.45E-08	1.81E-14	1.95E-08	2.77E+01	2.77E+01	2.77E+01	2.01E+09
F31	6.01E+09	1	2.00E+01	4.73E-08	0.00E+00	1.82E-08	2.00E+01	2.00E+01	2.00E+01	1.55E+09
F20	1.04E+09	1	4.37E+00	4.87E-08	3.37E-12	2.29E-08	4.37E+00	4.37E+00	4.37E+00	2.69E+08
F17	-9.87E+08	0	-2.03E+00	1.96E-08	4.52E-16	1.13E-08	-2.03E+00	-2.03E+00	-2.03E+00	-2.55E+08
F21	-8.90E+08	0	-1.66E+00	1.75E-08	1.50E-12	1.02E-08	-1.66E+00	-1.66E+00	-1.66E+00	-2.30E+08
F33	-4.08E+08	0	-1.53E+00	3.89E-08	1.26E-12	2.05E-08	-1.53E+00	-1.53E+00	-1.53E+00	-1.05E+08
F26	2.42E+08	1	6.66E-01	3.52E-07	1.55E-13	1.50E-08	6.66E-01	6.66E-01	6.66E-01	6.26E+07
F10	1.71E+05	1	1.25E+04	4.95E-08	4.01E-01	1.86E-08	1.25E+04	1.25E+04	1.25E+04	4.42E+04

Table 11. Top-10 functions by |Z| at D = 30 vs DMOA

Func	Z	p_one	mean_WFOA	mean_comp	sd_WFOA	sd_comp	mean_diff	CI95_low	CI95_high	Cohen_d
F34	-1.61E+16	0	-3.03E-05	5.22E-28	1.03E-20	2.25E-28	-3.03E-05	-3.03E-05	-3.03E-05	-4.15E+15
F19	-6.69E+08	0	-3.08E+01	3.43E-07	1.08E-14	2.52E-07	-3.08E+01	-3.08E+01	-3.08E+01	-1.73E+08
F22	5.79E+08	1	2.77E+01	3.21E-07	1.81E-14	2.62E-07	2.77E+01	2.77E+01	2.77E+01	1.49E+08
F31	4.83E+08	1	2.00E+01	3.92E-07	0.00E+00	2.27E-07	2.00E+01	2.00E+01	2.00E+01	1.25E+08
F17	-2.67E+08	0	-2.03E+00	5.39E-08	4.52E-16	4.18E-08	-2.03E+00	-2.03E+00	-2.03E+00	-6.88E+07
F26	1.76E+08	1	6.66E-01	1.08E-04	1.55E-13	2.07E-08	6.66E-01	6.66E-01	6.66E-01	4.55E+07
F20	9.74E+07	1	4.37E+00	3.49E-07	3.37E-12	2.46E-07	4.37E+00	4.37E+00	4.37E+00	2.51E+07
F21	-8.70E+07	0	-1.66E+00	1.28E-07	1.50E-12	1.05E-07	-1.66E+00	-1.66E+00	-1.66E+00	-2.25E+07
F33	-3.62E+07	0	-1.53E+00	3.44E-07	1.26E-12	2.31E-07	-1.53E+00	-1.53E+00	-1.53E+00	-9.35E+06
F10	1.71E+05	1	1.25E+04	2.67E-07	4.01E-01	2.36E-07	1.25E+04	1.25E+04	1.25E+04	4.42E+04

Table 12. Top-10 functions by |Z| at D = 50 vs CMOA

Func	Z	p_one	mean_WFOA	mean_comp	sd_WFOA	sd_comp	mean_diff	CI95_low	CI95_high	Cohen_d
F34	-1.61E+16	0	-3.03E-05	1.55E-24	1.03E-20	1.95E-24	-3.03E-05	-3.03E-05	-3.03E-05	-4.15E+15
F19	-1.07E+10	0	-3.08E+01	3.81E-08	1.08E-14	1.57E-08	-3.08E+01	-3.08E+01	-3.08E+01	-2.76E+09
F22	9.87E+09	1	2.77E+01	3.42E-08	1.81E-14	1.54E-08	2.77E+01	2.77E+01	2.77E+01	2.55E+09
F31	7.38E+09	1	2.00E+01	3.02E-08	0.00E+00	1.48E-08	2.00E+01	2.00E+01	2.00E+01	1.91E+09
F27	-2.09E+09	0	-1.24E+02	2.45E-08	3.24E-07	1.33E-08	-1.24E+02	-1.24E+02	-1.24E+02	-5.39E+08
F20	1.97E+09	1	4.37E+00	2.70E-08	2.81E-12	1.21E-08	4.37E+00	4.37E+00	4.37E+00	5.09E+08
F17	-1.34E+09	0	-2.03E+00	1.05E-08	4.52E-16	8.30E-09	-2.03E+00	-2.03E+00	-2.03E+00	-3.47E+08
F21	-1.05E+09	0	-1.66E+00	1.65E-08	5.95E-13	8.64E-09	-1.66E+00	-1.66E+00	-1.66E+00	-2.72E+08
F33	-5.46E+08	0	-1.53E+00	2.71E-08	1.12E-12	1.53E-08	-1.53E+00	-1.53E+00	-1.53E+00	-1.41E+08
F26	1.83E+08	1	6.66E-01	3.40E-07	1.52E-13	1.99E-08	6.66E-01	6.66E-01	6.66E-01	4.72E+07

Table 13. Top-10 functions by |Z| at D = 50 vs DMOA

Func	Z	p_one	mean_WFOA	mean_comp	sd_WFOA	sd_comp	mean_diff	CI95_low	CI95_high	Cohen_d
F34	-1.61E+16	0	-3.03E-05	7.10E-28	1.03E-20	3.34E-28	-3.03E-05	-3.03E-05	-3.03E-05	-4.15E+15
F27	-1.66E+09	0	-1.24E+02	2.99E-07	3.24E-07	2.46E-07	-1.24E+02	-1.24E+02	-1.24E+02	-4.30E+08
F22	6.06E+08	1	2.77E+01	2.64E-07	1.81E-14	2.50E-07	2.77E+01	2.77E+01	2.77E+01	1.56E+08
F19	-5.85E+08	0	-3.08E+01	3.60E-07	1.08E-14	2.88E-07	-3.08E+01	-3.08E+01	-3.08E+01	-1.51E+08
F31	3.40E+08	1	2.00E+01	4.14E-07	0.00E+00	3.22E-07	2.00E+01	2.00E+01	2.00E+01	8.78E+07
F17	-1.98E+08	0	-2.03E+00	6.91E-08	4.52E-16	5.62E-08	-2.03E+00	-2.03E+00	-2.03E+00	-5.12E+07
F26	1.87E+08	1	6.66E-01	1.08E-04	1.52E-13	1.95E-08	6.66E-01	6.66E-01	6.66E-01	4.82E+07
F21	-8.49E+07	0	-1.66E+00	1.48E-07	5.95E-13	1.07E-07	-1.66E+00	-1.66E+00	-1.66E+00	-2.19E+07
F20	8.29E+07	1	4.37E+00	3.89E-07	2.81E-12	2.89E-07	4.37E+00	4.37E+00	4.37E+00	2.14E+07
F33	-3.24E+07	0	-1.53E+00	3.24E-07	1.12E-12	2.59E-07	-1.53E+00	-1.53E+00	-1.53E+00	-8.36E+06

Table 14. Top-10 functions by |Z| at D = 100 vs CMOA

Func	Z	p_one	mean_WFOA	mean_comp	sd_WFOA	sd_comp	mean_diff	CI95_low	CI95_high	Cohen_d
F34	-1.61E+16	0	-3.03E-05	4.93E-28	1.03E-20	3.04E-28	-3.03E-05	-3.03E-05	-3.03E-05	-4.15E+15
F22	6.92E+08	1	2.77E+01	2.54E-07	1.81E-14	2.19E-07	2.77E+01	2.77E+01	2.77E+01	1.79E+08
F19	-5.32E+08	0	-3.08E+01	3.89E-07	1.08E-14	3.17E-07	-3.08E+01	-3.08E+01	-3.08E+01	-1.37E+08
F31	4.32E+08	1	2.00E+01	2.80E-07	0.00E+00	2.53E-07	2.00E+01	2.00E+01	2.00E+01	1.12E+08
F17	-2.47E+08	0	-2.03E+00	4.77E-08	4.52E-16	4.51E-08	-2.03E+00	-2.03E+00	-2.03E+00	-6.38E+07
F26	1.85E+08	1	6.66E-01	1.08E-04	1.00E-13	1.97E-08	6.66E-01	6.66E-01	6.66E-01	4.78E+07
F20	1.68E+08	1	4.37E+00	1.95E-07	2.06E-12	1.43E-07	4.37E+00	4.37E+00	4.37E+00	4.33E+07
F21	-1.13E+08	0	-1.66E+00	1.03E-07	9.65E-13	8.05E-08	-1.66E+00	-1.66E+00	-1.66E+00	-2.92E+07
F33	-3.05E+07	0	-1.53E+00	4.20E-07	7.15E-13	2.74E-07	-1.53E+00	-1.53E+00	-1.53E+00	-7.88E+06

Table 15. Top-10 functions by |Z| at D = 100 vs DMOA

Func	Z	p_one	mean_WFOA	mean_comp	sd_WFOA	sd_comp	mean_diff	CI95_low	CI95_high	Cohen_d
F34	-1.61E+16	0	-3.03E-05	4.93E-28	1.03E-20	3.04E-28	-3.03E-05	-3.03E-05	-3.03E-05	-4.15E+15
F22	6.92E+08	1	2.77E+01	2.54E-07	1.81E-14	2.19E-07	2.77E+01	2.77E+01	2.77E+01	1.79E+08
F19	-5.32E+08	0	-3.08E+01	3.89E-07	1.08E-14	3.17E-07	-3.08E+01	-3.08E+01	-3.08E+01	-1.37E+08
F31	4.32E+08	1	2.00E+01	2.80E-07	0.00E+00	2.53E-07	2.00E+01	2.00E+01	2.00E+01	1.12E+08
F17	-2.47E+08	0	-2.03E+00	4.77E-08	4.52E-16	4.51E-08	-2.03E+00	-2.03E+00	-2.03E+00	-6.38E+07
F26	1.85E+08	1	6.66E-01	1.08E-04	1.00E-13	1.97E-08	6.66E-01	6.66E-01	6.66E-01	4.78E+07
F20	1.68E+08	1	4.37E+00	1.95E-07	2.06E-12	1.43E-07	4.37E+00	4.37E+00	4.37E+00	4.33E+07
F21	-1.13E+08	0	-1.66E+00	1.03E-07	9.65E-13	8.05E-08	-1.66E+00	-1.66E+00	-1.66E+00	-2.92E+07
F33	-3.05E+07	0	-1.53E+00	4.20E-07	7.15E-13	2.74E-07	-1.53E+00	-1.53E+00	-1.53E+00	-7.88E+06
F10	1.17E+05	1	4.18E+04	2.84E-07	1.95E+00	2.32E-07	4.18E+04	4.18E+04	4.18E+04	3.03E+04

7 Potential Applications

Many different fields where complex optimization is required show great promise for the Water Flow Optimization Algorithm (WFOA). The algorithm is based on how natural water flows, so it combines flow dynamics to efficiently explore the search space with strong exploitation through potential gradients and transpiration mechanisms that cause convergence. This balance is particularly attractive for nonlinear, multimodal, and high-dimensional problems whose conditions may change over time [48-49].

One natural application domain is engineering design. Many design tasks—such as structural sizing, fluid and thermal systems, energy devices, or material selection—lead to models with strong nonlinearities and several local optima. In such cases, WFOA can be used to search for lighter structural components, more efficient mechanical systems, or energy devices that operate with better performance-cost trade-offs. Because of its population-based nature, the method can deliver outstanding candidate designs while keeping the computational effort at a reasonable level compared with traditional approaches [50].

While this paper focuses on benchmark tests, we can apply the same principles to industrial and manufacturing environments. In production systems, for example, WFOA could assist in building production schedules, assigning machines or workers to specific tasks, and

supporting routine supply-chain decisions. The water-flow analogy is easy to interpret: resources are gradually redirected to stages where they are more useful so that production costs are reduced and idle time is minimized.

In a similar way, WFOA might be embedded in routing and vehicle-assignment procedures or in flow-management policies for logistics and transportation networks that must operate under changing demand and capacity constraints [51-52].

Energy systems and sustainability provide another promising field. Modern energy infrastructures must deal with uncertainty, nonlinear dynamics, and the integration of renewable sources. Optimization tools are required to locate new renewable units, configure microgrids, schedule storage devices, or design control strategies for smart grids. WFOA could be used as the core search engine in these tasks, for instance, to choose placements of solar or wind farms, tune controllers that minimize losses, or plan how electricity is routed through a network with variable demand.

The algorithm is also useful for applications that use data, like data science and machine learning. You could use it for feature selection, tuning model parameters, clustering, or training neural networks. In these situations, WFOA can help keep a wide range of candidate models while avoiding early convergence. This technique is especially useful when there are a lot of features or parameters [53].

In structural and mechanical engineering, WFOA could be used with Finite Element Method (FEM) solvers to make complex parts work better when they are hit, worn out, or stiff. For example, recent research has demonstrated the efficacy of integrating optimization algorithms with FEM to enhance the crashworthiness of vehicle monocoque structures [54]. WFOA could also be used to identify designs that are strong and light and meet a number of performance criteria.

WFOA can be used for more than just classical numerical benchmarks; it can also be used for data-driven applications. Nature-inspired metaheuristics have been effectively utilized in tasks such as the selection of content measures for text summary evaluation through genetic algorithms [55]. The evidence indicates that WFOA may be modified for feature selection, text mining, or other high-dimensional challenges characterized by a complex and non-convex search space.

The configuration of WFOA implies its potential application across diverse fields. For example, in bioinformatics, it could help with drug design pipelines, choosing genes or features, or sequence alignment tasks where the search space is high-dimensional and noisy.

Since it is based on how water moves, it is a beneficial choice for planning how to distribute water, control pollution, or manage land use. In healthcare, WFOA could be used in treatment planning, medical image analysis, or decision support systems that need strong optimization when there is uncertainty.

These possibilities suggest that WFOA should not be regarded solely as an instrument for synthetic benchmark functions. Instead, it can be considered a flexible optimization framework that can change based on different modeling assumptions and limits.

Its biologically inspired search method, which is based on the flow of solutions toward promising areas, makes it strong enough to work in landscapes that are irregular and have multiple modes. For these reasons, we think that WFOA has a favorable chance of being used as an optimization engine in both future academic research and real-world business applications.

8 Conclusions and Future Work

This paper presented the Water Flow Optimization Algorithm (WFOA), a bio-inspired metaheuristic based on the physiology of water transport in plants, where water potential gradients facilitate upward flow from roots to leaves [36, 38-39]. The algorithm's simple, flow-based update finds a balance between exploration and exploitation without using more than one operator, which is in line with well-known rules for parameter control and simplicity in evolutionary computation [40-50].

We tested WFOA on 36 classical test mathematic functions with fixed evaluation budgets and 30 runs for each function and dimension. CMOA and DMOA were used as starting points for comparative analyses. The results in Tables 3–6 and Figures 1–6 show that WFOA is competitive on unimodal/separable problems and consistently does better on several multimodal landscapes. The statistical package includes a left-tailed Z-test ($\alpha = 0.05$), a mean difference (Δ), a one-tailed p-value, Cohen's d, BH–FDR control, and WinRate. These provide you both a way to discover things and a way to see how they affect you in real life.

We believe that WFOA's simplicity and flexibility make it an outstanding choice for varied optimization environments in engineering and data analysis, where reliable executions and easy implementation are important [50-53].

9 Future Work

Control of adaptive parameters. To make convergence even more stable and avoid getting stuck too soon, add dynamic schedules or feedback-driven adaptation for step-size and stochastic components [40, 50].

- Mixing. Look into how fuzzy logic systems and deep neural networks can work together as surrogate models or controllers. You could also look into how they can work with well-known metaheuristics (as separate ablation branches [50-55]).
- This study examines fixed control parameters; however, numerous studies have shown that parameter adaptation can substantially enhance

the performance and robustness of nature-inspired algorithms. In particular, fuzzy-based schemes have been successfully integrated into metaheuristics to adjust their behavior during the search [56-58]. As future work, WFOA could incorporate fuzzy or adaptive controllers for its flow and transpiration coefficients, potentially improving convergence speed and solution quality.

- Another promising research direction is the development of multi-objective variants of WFOA. Recent approaches based on particle swarm optimization have proposed sophisticated mechanisms to handle conflicting objectives and approximate Pareto fronts in complex scenarios [57]. Inspired by these ideas, a multi-objective WFOA could be designed to balance several criteria simultaneously, making the algorithm suitable for engineering and real-world problems where trade-offs between objectives are unavoidable.
- Variants that are both multi-objective and discrete. To make it more useful for real-world design and routing problems, add Pareto-based selection and combinatorial encodings (through discrete or integer mappings) to the flow operator [51-53].
- Dealing with constraints. To improve performance on engineering tasks with limited resources, use moves that keep feasibility and penalty/repair strategies [50-53].
- The ability to grow. Evaluate behavior in extensive continuous environments (hundreds to thousands of variables) and examine memory/runtime profiles under constrained budgets [51-53].
- More validation. Add new, larger benchmarks to the current suite and use case studies from fields like energy systems, logistics, and bioinformatics to show that the results are valid outside of the lab [50-53].
- Being able to be repeated. Make a public code repository and parameter files available so that others can check your work and use it again later.

In short, WFOA has a simple but effective search tool based on plant hydraulics that works well in many different settings and is easy to set up

and tweak. The steps above show a good way to make things more general and have a bigger effect in both academic and business settings.

References

1. **Yang, X.-S. (2014).** Nature-Inspired Optimization Algorithms. Elsevier.
2. **Mirjalili, S. (2019).** Evolutionary Algorithms and Metaheuristics. Springer.
3. **Holland, J.H. (1975).** Adaptation in Natural and Artificial Systems. University of Michigan Press.
4. **Said, Y., Ayachi, R., Afif, M., Saidani, T., Alanezi, S.T., Saidani, O., Algarni, A.D. (2025).** AI-Driven Genetic Algorithm-Optimized Lung Segmentation for Precision in Early Lung Cancer Diagnosis. *Scientific Reports*, Vol. 15, pp. 23058. doi: 10.1038/s41598-025-08116-w.
5. **Meniz, B., Tiryaki, F. (2024).** Genetic Algorithm Optimization with Selection Operator Decider. *Arabian Journal for Science and Engineering*. doi: 10.1007/s13369-024-09068-5.
6. **Katoch, S., Chauhan, S.S., Kumar, P. (2021).** A Review on Genetic Algorithm: Past, Present, and Future. *Multimedia Tools and Applications*, Vol. 80, No. 5, pp. 8091–8126. doi: 10.1007/s11042-020-10139-6.
7. **Hassan, H.E., Ibrahim, K.H., Madian, A.H. (2025).** Optimizing Multiprocessor Performance in Real-Time Systems Using an Innovative Genetic Algorithm Approach. *Scientific Reports*, Vol. 15, pp. 3842. doi: 10.1038/s41598-024-80910-4.
8. **Kennedy, J., Eberhart, R. (1995).** Particle Swarm Optimization. In *Proceedings of the IEEE International Conference on Neural Networks*.
9. **Jakšić, Z., Devi, S., Jakšić, O., Guha, K. (2023).** A Comprehensive Review of Bioinspired Optimization Algorithms Including Applications in Microelectronics and Nanophotonics. *Biomimetics*, Vol. 8, No. 3, pp. 278. doi: 10.3390/biomimetics8030278.
10. **Caselli, N., Soto, R., Crawford, B., Valdivia, S., Chicata, E., Olivares, R. (2024).** Dynamic

- Population on Bio-Inspired Algorithms Using Machine Learning for Global Optimization. *Biomimetics*, Vol. 9, No. 1, pp. 7. doi: 10.3390/biomimetics9010007.
11. **Cao, W., Tan, Y., Huang, M., Luo, Y. (2020).** Adaptive Bacterial Foraging Optimization Based on Roulette Strategy. In *Advances in Swarm Intelligence*, pp. 299–311. Springer. doi: 10.1007/978-3-030-53956-6_27.
 12. **Dorigo, M., Gambardella, L.M. (1997).** Ant Colony System: A Cooperative Learning Approach to the Traveling Salesman Problem. *IEEE Transactions on Evolutionary Computation*, Vol. 1, No. 1, pp. 53–66.
 13. **Manthey, B., van Rhijn, J., Safari, A., Vredeveld, T. (2025).** Convergence and Running Time of Time-Dependent Ant Colony Algorithms. arXiv preprint arXiv:2501.10810.
 14. **Ye, H., Wang, J., Cao, Z., Liang, H., Li, Y. (2023).** DeepACO: Neural-Enhanced Ant Systems for Combinatorial Optimization. arXiv preprint arXiv:2309.14032.
 15. **Li, P., Wei, L., Wu, D. (2025).** An Intelligently Enhanced Ant Colony Optimization Algorithm for Global Path Planning of Mobile Robots in Engineering Applications. *Sensors*, Vol. 25, No. 5, pp. 1326. doi: 10.3390/s25051326.
 16. **Dorigo, M., Birattari, M., Stützle, T. (2024).** Ant Colony Optimization: A Bibliometric Review. *Physics of Life Reviews*, Vol. 52, pp. 213–230. doi: 10.1016/j.plrev.2024.11.015.
 17. **Karaboga, D., Basturk, B. (2007).** A Powerful and Efficient Algorithm for Numerical Function Optimization: Artificial Bee Colony (ABC) Algorithm. *Journal of Global Optimization*, Vol. 39, pp. 459–471.
 18. **Guo, H., Lai, X., Guo, J., You, G., Alnafrh, I. (2025).** An Improved Hybrid Artificial Bee Colony Algorithm for a Multi-Supplier Closed-Loop Location-Inventory Problem with Customer Returns. *PLoS ONE*, Vol. 20, No. 5, pp. e0324343. doi: 10.1371/journal.pone.0324343.
 19. **Ibrahim, A.O., Elbushra, E.M., Hashem, I.A.T., Syed, H.J., Ismail, M.A., Osman, A.H., Ahmed, A.A. (2025).** The Artificial Bee Colony Algorithm: A Comprehensive Survey of Variants, Modifications, Applications, Developments, and Opportunities. *Archives of Computational Methods in Engineering*. doi: 10.1007/s11831-025-10269-w.
 20. **Carreon-Ortiz, H., Valdez-Fevrier, V., Castillo, O. (2023).** Comparative Study of Type-1 and Interval Type-2 Fuzzy Logic Systems in Parameter Adaptation for the Fuzzy Discrete Mycorrhiza Optimization Algorithm. *Mathematics*, Vol. 11, No. 11, pp. 2501. doi: 10.3390/math11112501.
 21. **Carreon-Ortiz, H., Valdez, F., Castillo, O. (2022).** A New Discrete Mycorrhiza Optimization Nature-Inspired Algorithm. *Axioms*, Vol. 11, No. 8, pp. 391. doi: 10.3390/axioms11080391.
 22. **Carreon-Ortiz, H., Valdez-Fevrier, V., Castillo, O. (2023).** Conclusions of the Mycorrhiza Optimization Algorithm. In *Mycorrhiza Optimization Algorithm*, pp. 75–76. SpringerBriefs in Applied Sciences and Technology. doi: 10.1007/978-3-031-47369-2_7.
 23. **Mirjalili, S., Mirjalili, S.M., Lewis, A. (2014).** Grey Wolf Optimizer. *Advances in Engineering Software*, Vol. 69, pp. 46–61.
 24. **Dagal, I., Ibrahim, A.O., Harrison, A., Mbasso, W.F., Hourani, A.O., Zaitsev, I. (2025).** Hierarchical Multi-Step Gray Wolf Optimization (HMS-GWO) for Energy Systems Optimization. *Scientific Reports*, Vol. 15, pp. 8973. doi: 10.1038/s41598-025-92983-w.
 25. **Shaikh, M.S., Lin, H., Xie, S., Dong, X., Lin, Y., Shiva, C.K., Fendzi Mbasso, W. (2025).** An Intelligent Hybrid Grey Wolf-Particle Swarm Optimizer (HGWPSO) for Complex Engineering Design Problems. *Scientific Reports*, Vol. 15, pp. 18313. doi: 10.1038/s41598-025-02154-0.
 26. **Kirkpatrick, S., Gelatt, C.D., Vecchi, M.P. (1983).** Optimization by Simulated Annealing. *Science*, Vol. 220, No. 4598, pp. 671–680. doi: 10.1126/science.220.4598.671.
 27. **Milisav, F., Bazinet, V., Betzel, R.F., Mišić, B. (2025).** A Simulated Annealing Algorithm for Randomizing Weighted Networks. *Nature Computational Science*, Vol. 5, No. 1, pp. 48–64. doi: 10.1038/s43588-024-00735-z.

28. **Yu, V.F., Lin, C.-H., Maglasang, R.S., Lin, S.-W., Chen, K.-F. (2024).** An Efficient Simulated Annealing Algorithm for the Vehicle Routing Problem in Omnichannel Distribution. *Mathematics*, Vol. 12, No. 23, pp. 3664. doi: 10.3390/math12233664.
29. **Yang, X.-S. (2010).** Firefly Algorithm, Lévy Flights and Global Optimization. In *Research and Development in Intelligent Systems XXVI*. Springer.
30. **Rani, R., Sharma, S. (2025).** Evaluating the Suitability of the Firefly Algorithm for Optimization in Optical and IoT Networks. *Journal of Optical Communications*. doi: 10.1515/joc-2025-0262.
31. **Joy, G., Huyck, C., Yang, X.S. (2024).** Parameter Tuning of the Firefly Algorithm by Standard Monte Carlo and Quasi-Monte Carlo Methods. In *Computational Science – ICCS 2024*, LNCS 14836, pp. 242–253. Springer. doi: 10.1007/978-3-031-63775-9_17.
32. **Dao, T.-K., Nguyen, T.-T. (2024).** A Review of the Bat Algorithm and Its Varieties for Industrial Applications. *Journal of Intelligent Manufacturing*. doi: 10.1007/s10845-024-02506-z.
33. **Zhang, Q., Xing, Y., Yao, M., Wang, J., Guo, X., Qin, S., Qi, L., Huang, F. (2024).** An Improved Discrete Bat Algorithm for Multi-Objective Partial Parallel Disassembly Line Balancing Problem. *Mathematics*, Vol. 12, No. 5, pp. 703. doi: 10.3390/math12050703.
34. **Hammel, H.T., Scholander, P.F., Bradstreet, E.D., Hemmingsen, E.A. (1971).** Fine Structure and Function in Plant Water Relations. *Annual Review of Plant Physiology*, Vol. 22, pp. 255–277.
35. **Holbrook, N.M., Zwieniecki, M.A. (2005).** *Water Transport in Plants*. Academic Press.
36. **Taiz, L., Zeiger, E., Møller, I.M., Murphy, A. (2015).** *Plant Physiology and Development*. 6th ed. Sinauer Associates.
37. **Nobel, P.S. (2009).** *Physicochemical and Environmental Plant Physiology*. 4th ed. Academic Press.
38. **Tyree, M.T., Zimmermann, M.H. (2002).** *Xylem Structure and the Ascent of Sap*. 2nd ed. Springer-Verlag.
39. **Steudle, E. (2001).** The Cohesion–Tension Mechanism and the Acquisition of Water by Plant Roots. *Annual Review of Plant Biology*, Vol. 52, pp. 847–875. doi: 10.1146/annurev.arplant.52.1.847.
40. **Eiben, A.E., Hinterding, R., Michalewicz, Z. (1999).** Parameter Control in Evolutionary Algorithms. *IEEE Transactions on Evolutionary Computation*, Vol. 3, No. 2, pp. 124–141. doi: 10.1109/4235.771166.
41. **Fister, I., Yang, X.-S., Fister, I. Jr., Brest, J., Fister, D. (2013).** A Brief Review of Nature-Inspired Algorithms for Optimization. arXiv preprint arXiv:1307.4186.
42. **Karim, F.K., Rahman, M.M., Eid, M.M., Towfek, S.K., Alkahtani, H.K. (2023).** A Novel Bio-Inspired Optimization Algorithm Design for Wind Power Engineering Applications Time-Series Forecasting. *Biomimetics*, Vol. 8, No. 3, pp. 321. doi: 10.3390/biomimetics8030321.
43. **He, J., Tang, Y., Guo, X. et al. (2024).** Research on Hybrid Reservoir Scheduling Optimization Based on Improved Walrus Optimization Algorithm with Coupling Adaptive ϵ Constraint and Multi-Strategy Optimization. *Scientific Reports*, Vol. 14, pp. 11981. doi: 10.1038/s41598-024-62722-8.
44. **Zhao, Z., Luo, S. (2024).** A Crisscross-Strategy-Boosted Water Flow Optimizer for Global Optimization and Oil Reservoir Production. *Biomimetics*, Vol. 9, No. 1, pp. 20. doi: 10.3390/biomimetics9010020.
45. **Nguyen, T.H. et al. (2022).** Review of Bio-Inspired Optimization Applications in Renewable-Powered Smart Grids: Emerging Population-Based Metaheuristics. *Journal of Cleaner Production*, Vol. 364, pp. 132–146.
46. **Luo, K. (2022).** Water Flow Optimizer: A Nature-Inspired Evolutionary Algorithm for Global Optimization. *IEEE Transactions on Cybernetics*, Vol. 52, No. 8, pp. 7753–7764. doi: 10.1109/TCYB.2021.3049607.
47. **Ghasemi, M., Davoudkhani, I.F., Akbari, E., Rahimnejad, A., Ghavidel, S., Li, L. (2020).** Turbulent Flow of Water-Based Optimization (TFWO): A Novel and Effective Algorithm for Global Optimization and Its Engineering

- Applications. *Engineering Applications of Artificial Intelligence*, Vol. 92, pp. 103666.
48. **Liang, J.J., Qu, B.Y., Suganthan, P.N. (2013).** Problem Definitions and Evaluation Criteria for the CEC 2013 Special Session on Real-Parameter Optimization. Technical Report.
 49. **Awad, N.H., Ali, M.Z., Liang, J.J., Qu, B.Y., Suganthan, P.N. (2016).** Problem Definitions and Evaluation Criteria for the CEC 2017 Special Session and Competition on Single-Objective Real-Parameter Numerical Optimization. Technical Report. Nanyang Technological University.
 50. **Yang, X.-S. (2021).** *Nature-Inspired Optimization Algorithms*. 2nd ed. Elsevier.
 51. **Talbi, E.-G. (2009).** *Metaheuristics: From Design to Implementation*. Wiley.
 52. **Blum, C., Roli, A. (2003).** Metaheuristics in Combinatorial Optimization: Overview and Conceptual Comparison. *ACM Computing Surveys*, Vol. 35, No. 3, pp. 268–308. doi: 10.1145/937503.937505.
 53. **Boussaïd, I., Lepagnot, J., Siarry, P. (2013).** A Survey on Optimization Metaheuristics. *Information Sciences*, Vol. 237, pp. 82–117. doi: 10.1016/j.ins.2013.02.041.
 54. **Soto-Barrón, F.O., Romero-Ángeles, B., Guzmán-Baeza, M., Martínez-Reyes, J., Urriolagoitia-Calderón, G. (2024).** Optimization by the Finite Element Method of a Commercial Sedan Automobile Monocoque for Best Response to an Impact Collision. *Computación y Sistemas*, Vol. 28, No. 4, pp. 1799–1809. doi: 10.13053/CyS-28-4-4909.
 55. **Rojas-Simón, J., Ledeneva, Y., García-Hernández, R.A. (2024).** Selection of Content Measures for Evaluation of Text Summaries Using Genetic Algorithms. *Computación y Sistemas*, Vol. 28, No. 4, pp. 2261–2278. doi: 10.13053/CyS-28-4-5291.
 56. **Carreón-Ortiz, H., Valdez, F., Castillo, Ó. (2022).** Fuzzy Flower Pollination Algorithm: Comparative Study of Type-1 and Interval Type-2 Fuzzy Logic System in Parameter Adaptation Optimization. *Computación y Sistemas*, Vol. 26, No. 2, pp. 643–661. doi: 10.13053/CyS-26-2-4247.
 57. **Domínguez-Guerrero, J., Montiel-Ross, Ó., Carrillo, V., Martínez, E., Castillo, Ó. (2024).** Normal Attractor Intersection Based Multi-objective Optimization Using Particle Swarm Optimization. *Computación y Sistemas*, Vol. 28, No. 3, pp. 1613–1623. doi: 10.13053/CyS-28-3-5177.
 58. **Sanchez, D., Melin, P., Castillo, O. (2020).** Comparison of Particle Swarm Optimization Variants with Fuzzy Dynamic Parameter Adaptation for Modular Granular Neural Networks for Human Recognition. *Journal of Intelligent & Fuzzy Systems*, Vol. 38, No. 3, pp. 3229–3252. doi: 10.3233/JIFS-191198.

Articles received on 07/11/2025; accepted on 09/01/2026.

**Corresponding author is Fevrier Valdez.*